waterloopkundig laboratorium
delft hydraulics laboratory

Twente University

phosphate adsorption

report on literature study

R 1310-8

Decembre 1982

Twente University

phosphate adsorption

report on literature study

R 1310-8

Decembre 1982

Preface

This report is the result of a literature study to the adsorption desorption phenomena of phosphorus in natural systems.

Phosphorus is one of the key elements in eutropication problems. The phosphorus behaviour is not only influenced by biological processes, but also by chemical processes. Understanding of these chemical processes is necessary for modelling eutrophication processes.

This research was carried out by J. Taat of the department of chemical Technology of the Twente University, in coöperation with N.M. de Rooij of the Delft Hydraulics Laboratory.

The research is a part of the WABASIM project (WAter BASIn Model), which is carried out by the Environmental Hydraulics Branch of the Delft Hydraulics Laboratory in coöperation with and by assigment of the Environmental Section of the Deltadienst Rijkswaterstaat.

CONTENTS

		page
1	Modes of description of the phosphate adsorption.....	1
1.1	Precipitation reactions.....	1
1.2	Equilibrium reactions.....	1
1.2.1	General description.....	2
1.2.2	The release of hydroxyl ions.....	2
1.2.3	Infra-Red studies.....	4
1.3	The effects of surface charge upon adsorption.....	5
1.3.1	The envelope of surface charge.....	5
1.3.2	Explanations of measurements with the VSG-VSP model.....	8
1.4	Adsorption isotherms.....	9
1.4.1	Langmuir isotherm.....	9
1.4.2	Freundlich -and other isotherms.....	11
2	Proporties of the phosphate adsorption.....	12
2.1	Adsorption isotherms.....	12
2.2	Influence of ionic strength.....	13
2.3	Influence of silicate ions on phosphate adsorption.....	15
2.4	Kinetics of adsorption.....	16
2.5	Desorption isotherms.....	20
2.6	The influence of pH on phosphate sorption.....	24
2.7	Influence of the redoxpotential on phosphate sorption.....	25
2.8	Irreversible reactions.....	27

LITERATURE

FIGURES

1 Modes of description of the phosphate adsorption

In the literature a number of models has been used for the description of phosphate adsorption an hydrous oxides, soils and sediments. These models facilitate the conception and prediction of phosphate adsorption under various conditions.
In this chapter the following ways to describe the adsorption are presented:

1. precipitation reactions
2. equilibrium reactions
3. effects of surface charge
4. adsorption isotherms

1.1 Precipitation reactions

Kittrick and Jackson (1956) observed at high phosphate concentrations (1 mol/l) the formation of a discrete phase on the iron silicate greenalite[1]. They used electron microscopy in their study. The reaction was fast on colloidal iron (III) oxide particals and on thin aluminum hydroxide films (order of minutes at room temperature), but extremely slow on minerals. J.O. Nriagu (1972, 1976) presents the solubility of a large number. Fe-Ca-Mg- and Al phoshates. However, in the literature little attention has been paid to the kinetics of precipitation (Riemsdijk 1979, p2). Neither will kinetics aspects be discussed in this section, but implicitly this subject is dealt with in section 2.8.

1.2 Equilibrium reactions

A method of describing phosphate adsorption on hydrous oxides and soils is to picture adsorption as a number of surface equilibrium reactions. This approach allows an easy explanation of the influence of pH on phosphate adsorption and the concomittant change in surface charge and also of the release of hydroxyl ions upon phosphate adsorption.

1) The exact structure of greenalite is not known, but it is thought to be the iron analog of kaolinite.

1.2.1 General description

Prevailing groups at the solid surface are: $-O^-$, $-OH$ and $-OH_2^+$ groups. These groups are in equilibrium with the hydroxyl ions and protons in the water. (See Scheme 1.1 and table 1.1). Hence, the pH of the water influences the distribution between these groups. Also orthophosphate ions in the solution can interact with the surface groups. Two forms of binding at the surface can be envisaged: with one or two P-O bonds (mono and bi-dentate).
The reactions as presented by Breeuwsma and Lyklema (1973) show the relationship between adsorption, surface charge and release of hydroxyl ions.

$$Fe\ OH_2^+ + H_2PO_4^- \rightleftarrows Fe\ H_2PO_4 + H_2O \qquad R = 0 \qquad (1)$$

$$Fe\ OH_2^+ + H\ PO_4^{2-} \rightleftarrows Fe\ H\ PO_4^- + H_2O \qquad R = 0 \qquad (2)$$

$$Fe\ OH + H_2PO_4^- \rightleftarrows Fe\ H_2PO_4 + OH^- \qquad R = 1 \qquad (3)$$

$$Fe\ OH + H\ PO_4^{2-} \rightleftarrows Fe\ H\ PO_4^- + OH^- \qquad R = 1 \qquad (4)$$

Where R is the ratio of hydroxyl ions released and phosphate ions adsorbed.
Consequences of these reactions will be discussed in the following sections.

1.2.2 The release of hydroxyl ions

An experimental approach to test the equilibrium model is the measurement of the release of hydroxyl ions during phosphate adsorption. Of special interest is the influence of pH and surface coverage. We will present and discuss here some results from literature.
Lijklema (1978, 1980) gives R (moles OH^-/moles PO_4) as function of pH and extent of adsorption (fig. 1.1) for freshly precipitated $Fe(OH)_3$ suspensions [iron concentrations 0.5-5.0 m mol/l, 15 minutes equilibrium time, final P concentration 5-200 μ mol/l]. Figure 1.1 shows that the specific hydroxyl release increases with increasing pH. This is in accordance with reactions (1)-(4): at high pH reactions (3) and (4) predominate. R increases also with increasing surface coverage, which can be explained by assuming that positive sites are occupied with priority. An interesting feature is that at pH = 8.5 R is greater then unity, obviously because also bidendate bonds were formed (cf. reactions β in scheme 1.1).
Breeuwsma and Lyklema (1973), using hematite (α - Fe_2O_3) also found an increasing R with pH (fig. 1.2). However, according these authors R is indepen-

dent of the final phosphate concentration. They measured at high P concentrations (initial 2000, final C. 1000-1900 μ mol/l) corresponding to the flattening of Lijklema's curves at higher surface coverage (= high final P concentration).

Ryden cs. (1977B) describe phosphate adsorption by three Langmuir equations[1]. Figure 1.3 shows some interesting results of their experimental work. They explain these results by means of equilibrium reactions. At low surface occupation no OH^- is released (pH constant). The uptake of Na^+ indicates that the surface charge has been lowered by adsorption. This is in accordance with reaction (1). At higher surface coverage OH^- is released and the surface charge is constant (according to reaction (3)). These observations were made both with Fe-gels and with soils.

Rayan (1974) identified phosphate reactive sites on hydrous alumina by measuring proton consumption during phosphate adsorption. Figure 1.4.A and 1.4.B show the results of his measurements. R increases with increasing surface coverage. At maximum surface occupation[2] the mechanism of adsorption changes and R drops from larger then 1 to about 0.5. Ryden suggests that after nearly complete displacement of OH_2^+ and -OH groups the Al-$\overset{H}{O}$-Al bonds are broken up. Rayan gives the following equations.

$$Al\text{-}\overset{H}{O}\text{-}Al + H_2PO_4^- \rightleftarrows Al - H_2PO_4^{-\frac{1}{2}} + Al - OH^{-\frac{1}{2}}$$

$$Al - OH^{-\frac{1}{2}} + H^+ \rightleftarrows Al - OH_2^{+\frac{1}{2}}$$

$$\underline{Al - OH^{+\frac{1}{2}} + H_2PO_4^- \rightleftarrows Al - H_2PO_4^{-\frac{1}{2}} + H_2O} +$$

$$Al\overset{H}{O}Al + H^+ + 2\,H_2PO_4^- \rightleftarrows 2\,Al - H_2PO_4^{-\frac{1}{2}} + H_2O$$

Hence, R = 0.5 (see also section 1.2.3, page 4).

At high pH Rayan found R to be constant until adsorption of about 200 μ mol phosphate/g hydrous oxide, with R = 1.44 (pH = 8.5, PZC = 9.3).

Beyond 200 μ mol/g R = 1.07 (see fig. 1.4.C). Rayan explains the difference between his results by assuming that at higher pH bidentate bonds are formed

1) See also section 1.4.1.
2) Defined by the Langmuir equation.

(reactions β in scheme 1.1, see also scheme 1.2).

1.2.3 Infra-Red studies

A direct method to investigate the bond between phosphate and the oxide or soil surface is IR spectophotometry. In this way Atkinson (1972) and Parfitt (1975, 1977, 1979) tried to identify the adsorbed phosphate on hematite (α-Fe_2O_3), goethite (α FeOOH), β FeOOH, lepidocrocile (γ FeOOH), irongels, gibbsite ($Al(OH)_3$) and clay.
The results of their work indicate that phosphate is adsorbed by ligand exchange with sigly coordinated -OH groups resulting in a bridging-binuclear complex (See reactions β in scheme 1.1). Parfitt (1979) is of the opninion that only bidentate bonds are formed: "There is no evidence for more than one adsorption mechanism for phosphate on goethite" (for adsorption below the adsorption maximum). This is not necessarily in disagreement with the results of section 1.2.2. Beek and van Riemsdijk (1979) give the following equations for the phosphate adsorption:

$$\text{surface} + a\ PO_4H_y \rightarrow \text{surface} \sim P + b\ H_2O + r\ OH^-$$

charge:

$$sx \qquad a(y-3) \qquad sx + (y-3) + r \qquad -r$$

or in case of formation of bidentate bonds:

$$\frac{s}{a}\ M\ OH_{\left(\frac{3}{2}+x\right)} + PO_4H_y \rightarrow M\ O_2PO_2H_{y'} + \left(\frac{s}{a}-2\right)\ M\ OH_{\frac{3}{2}+x'} + R\ OH + (2-R)\ H_2O$$

If $\Delta x = (x-x')$ and $\Delta y = (y-y')$ are zero (no change of dissociation upon adsorption, which implies that R is constant during adsorption):
$R = 1-2x$ and R ranges between 0($x=1/2$) and 2($x=-1/2$). The R value of 1.44 near the point of zero charge ($x=a$) indicates that $[(a/s-2)\ \Delta x + \Delta y] > 0$. If $s/a \leq 2$ then $\Delta x < 0$ and/or $\Delta y > 0$, which agrees with the assumption that positive sites are preferred. Hence it is also possible to explain the results of section 1.2.2 with a binuclear reaction.

1.3 The effects of surface charge upon adsorption

The equilibrium theory can be combined with electrostatic models. This approach releases the necessity to assume surface groups with different reactivity. It is also possible to predict the influence of non specific adsorbing (indifferent) ions, pH, id. on the extent of adsorption.
Surface chemists (like Levine and Smith (1971)) developed models describing the enveloped models describing the envelope of the surface potential. The theory presented in the next paragraph is an application of these models by Bowden and co-workers (1973, 1977).

1.3.1 The envelope of surface charge

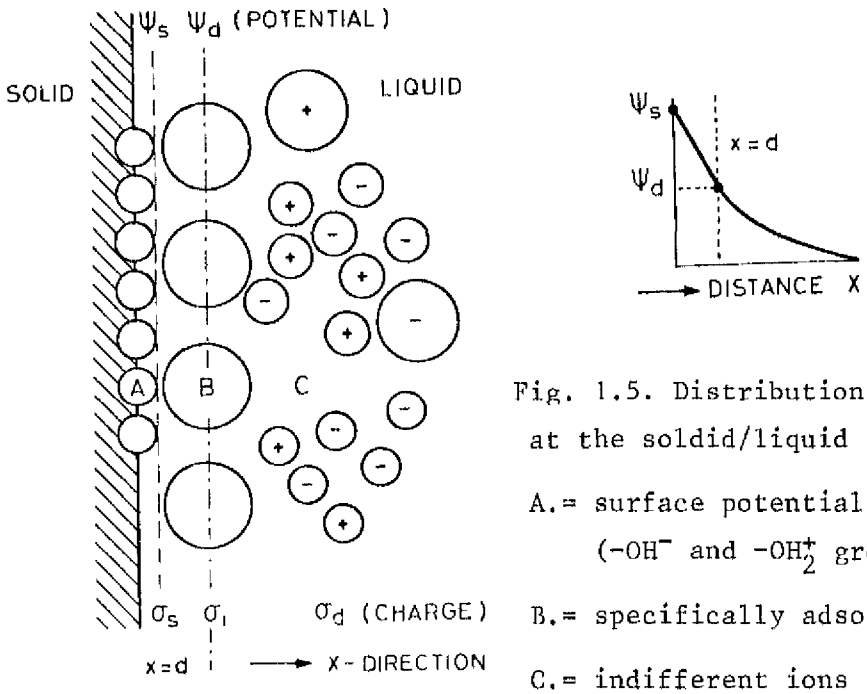

Fig. 1.5. Distribution of ions and potential at the soldid/liquid insterface.

A.= surface potential determining ions ($-OH^-$ and $-OH_2^+$ groups)

B.= specifically adsorbed ions ($PO_4^{\equiv}$, Ca^{+++} etc.)

C.= indifferent ions

Figure 1.5 shows the solid-liquid interface according to the Stern (1924) model. Potential determining ions are adsorbed at the solid surface (eg. H^+ and OH^- ions) The surface potential is ϕ_s, the surface charge is σ_s. The first layer at the surface contains specifically adsorbed ions (eg. $H\,PO_4^{2-}$, Ca^{2+} etc). The potential at this plane is ϕ_d, the surface charge density is σ_c. The second layer is the diffuse double layer with indifferent ions. The potential is a function of the distance x from the surface, the surface charge density is σ_d.
Now a set of equations can be derived defining the system. First the surface

charge is computed. The electrochemical potential of an ion i in the solution is:

$$\mu_i = \mu_i^o + RT \ln a_i$$

μ_i^o : is the chemical potential of ion i in standard state
R : gas constant
T : absolute temperature
a_i : activity of ion i in solution

The electro chemical potential of an ion i at the surface is:

$$\mu_{is} = \mu_{is}^o + RT \ln a_{is} + z_i F \psi_s + \Phi_i$$

index s : at the surface
z_i : valency ion i
F : Faranday constant
Φ : self atmosphere potential (due to the discretenes of charge, see Levine and Smith (1971), or for a review of this effect: Levine, Minquis and Bell (1967)).

At equilibrium is $\mu_i = \mu_{is}$, and substituting

$$K_i = \exp\left[(\mu_i^o - \mu_{is}^o - \Phi_i)/RT\right]$$

we obtain

$$a_{is} = K_i a_i \exp(-z_i F \psi_s/RT) \qquad (1.1)$$

The activity of the ion at the surface is controlled by the activity in the solution, by the constant K_i (Φ_i is concidered to be constant: $\mu_i^o - \mu_{is}^o - \Phi_i$ is the Stern potential ψ_i describing the chemical interaction between the surface and the ion) and by the electric potential at the surface. Consider the following reactions affecting the surface charge:

$$M \begin{matrix} OH \\ OH_2 \end{matrix}]^o + H^+ \underset{\leftarrow}{\overset{K_4}{\rightleftharpoons}} M \begin{matrix} OH_2 \\ OH_2 \end{matrix}]^+$$

$$M \begin{matrix} OH \\ OH_2 \end{matrix}]^o + OH^- \underset{\leftarrow}{\overset{K_{OH}}{\rightleftharpoons}} M \begin{matrix} OH \\ OH \end{matrix}]^- + H_2O$$

If the difference of surface concentrations $\Gamma_H - \Gamma_{OH}$ equals the surface charge σ_s and the H^+ and OH^- ions compete for N_s surface sites application of equation 1.1 yields:

$$\sigma_s = \frac{N_s[K_H a_H \exp(-F\ \psi_s/RT) - K_{OH} a_{OH} \exp\ (F\ \psi_s/RT)]}{1 + K_H a_H \exp(-F\ \psi_s/RT) + K_{OH} a_{OH} \exp\ (F\ \psi_s/RT)} \tag{1.2}$$

In the innermost plane of adsorption only specific adsorption occurs and for non-specific ions $K_i = 0$. The charge in the second layer is:

$$\sigma_i = \frac{N_t \Sigma(z_i K_i C_i \exp(-z_i\ F\ \psi_d/RT)}{1 + \Sigma(K_i C_i \exp(-z_i\ F\ \psi_d/RT)} \tag{1.3}$$

Where N_t is the maximum number that can be adsorbed in the first plane, C_i is the mole fraction of ion i (about 0.018 mole concentration, 25 C°, activity coefficients unity).

The charge in the diffuse layer is given by the Couy-Chapman theory (See Overbeek (1952):

$$\sigma_d = -1.22\ 10^{-10}\ \sqrt{C}\ \sinh\ (0.0195\ \ Z\ \ \psi_d) \tag{1.4}$$

Conditions: t = 25° C, C is the total ionic concentration in moles/l, charge of anions and cations are distributed symmetrically, ψ_d is expressed in mV. Between the surface and the layer with specific adsorbed ions there is no charge and the dielectric permittivity is supposed to be constant. According to Gauss' law:

$$(\psi_s - \psi_d) = (4\pi\ d/\varepsilon_d)\ \sigma_s = \sigma_s/G \tag{1.6}$$

in which d is the distance between the surface and the first layer (fig. 1.5), ε_d is the local permittivity ($0 < x < d$) and G is the capacitance of $0 < x < d$.

The system now has been defined: five variables (σ_s, σ_1, σ_d, ψ_s, ψ_d) and five equations (1.2-1.6). The four parameters N_s, K_H, K_{OH} and G can be obtained from titration curves. The fixed parameter N_T and the constants K_1 must be estimated when specific adsorption takes place.

1.3.2 Explanations of measurements with the VSG-VSP model

The variable-surface-charge variable-surface-potential (VSC-VSP) model, described in 1.3.1, is used to explain some experimental results, see figure 1.6.A and 1.6.B from a paper by Bowden cs(1973).

Only one value for N_T (the number of sites for specific adsorbed ions) has been used. The model predicts a change in binding energy if the change of the surface varies either through a change of pH or by adsorption. Therefore it is not necessary to postulate different types of sites, in contrast to the description in 1.2. Also the inflections at $pH = pK_{1o}$ (K_{1o} = ionisation constant of a weak acid or base, see fig. 1.7 form Hingston (1972)) are explained without specification of any special mechanism.

Hingstons explanation is in terms of work required to remove a proton from the undissociated acid, Breeuwsma (1973) comments this to be in conflict with elementary physical-chemical laws.

Anderson and Malotky (1979) use a model similar to that of Bowden. They measured the iso-electric point ($\psi_d \approx \psi_\xi = 0$[1]) at different phosphate surface coverages. The theory is in good agreement with the measurements (fig. 1.8).

A single value for both the affinity of adsorption Φ_a and the maximum adsorption Γ_{max} has been used, although their measurements cover a large range of phosphate concentrations (at equilibrium 0.01-100 μ mol/l). The constant Φ_a and Γ_{max} values also imply that it is unnecessary to differentiate between mono- and bidentate sites in order to model these modes of adsorption.

Brinkman (1979) presented a more sophisticated multi-layer model, in which the

1) The ξ potential (ψ_ξ) is the potential difference over the mobile part of the double layer, and can be measured by electrophoresis (see Overbeek, 1952, pg. 78).

dielectric permittivity is a function of the electric-field intensity. He defined different adsorption sites for the simulation of the surface charge at variable pH and KCl concentrations. A good agreement with measurements of Breeuwsma (1973) could be achieved.

1.4 Adsorption isotherms

A more or less empirical approach is the use of adsorption isotherms for the description of phosphate adsorption. The principal difference between the various isotherms is in the assumptions on the relationship between binding energy and the degree of surface occupation.

1.4.1 Langmuir isotherm

Langmuir assumed a limited number of localised adsorption sites at the surface in equilibrium with one molecular species in the solution:

$$E + C \overset{\rightarrow}{\leftarrow} EC \qquad \text{(only one molecule adsorbes at one site)}$$

E = an empty site at the surface
C = a molecule in the solution
EC = a molecule adsorbed

The activities are:

$$\{E\} = \gamma_E \, \Gamma_E / d$$

$$\{C\} = \gamma_C \, [C]$$

$$\{EC\} = \gamma_{EC} \, \Gamma_{EC} / d$$

γ_i = activity coefficient of species i
Γ_i = surface concentration i
d = layer thickness

At equilibrium:

$$K_{ads} = \exp(-\Delta G_{ads}/RT) = \frac{\{EC\}}{\{E\}\{C\}} = \frac{\gamma_{EC}\Gamma_{EC}/d}{\gamma_E\gamma_C\Gamma_E[C]/d}$$

substitute:

$$\Gamma_E = \Gamma_{max} - \Gamma_{EC}$$

and

$$\theta = \Gamma_{EC}/\Gamma_{max}$$

ΔG_{ads} = Gibbs free energy of adsorption
K_{ads} = equilibrium constant
Γ_{max} = maximum surface concentrations of adsorbed molecules
θ = fraction of occupied sites

and assume

$$\gamma_{EC} = \gamma_E$$

then:

$$\theta = \frac{K_{ads}}{1 + K_{ads}\{C\}}$$

This is the Langmuir isotherm, which can also be formulated as:

$$\frac{1}{x} = \frac{1}{(K_{ads} b\{C\})} + \frac{1}{b}$$

$b = \theta/x$ = adsorption max.
x = amount adsorbed

K_{ads} is considered not to be a function of θ and therefore ΔG_{ads} must be constant too. This means that:

a. all the adsorption sites have the same binding energy

b. the adsorbed molecules do not interact.

1.4.2 Freundlich - and other isotherms

Assuming that the affinity for adsorption decreases exponentially with the amount adsorbed one can derive the Freundlich equation (Ponec cs. 1974):

$$x = k\{C\}^{1/n}$$

where n and k are constants. This equation has been used succesfully (see chapter II) in the description of phosphate adsorption within a limited range of phosphate concentrations.

The Temkin equation has been derived with the assumption of a linear decrease in affinity of adsorption with increasing amount adsorbed:

$$x = k_1 \ln(k_2 \ln\{C\})$$

where k_1 and k_2 are constants. Further, mainly empirical extensions of these isotherms have been proposed. For instance, the observation that the amount of adsorbed phosphate increases continuously with increasing phosphate concentrations, led to an extended Langmuir equation:

$$\frac{\{C\}}{x} = A + B\{C\} + D\sqrt{\{C\}}$$

where A, B and D are constants. This equation does not predict a maximum adsorption, as the Langmuir isotherm does.
The Freundlich isother is often justified for firmly adsorbed phosphate, that was already present before the beginning of the experiment (e.g. in soils)

$$x = k\ C^{1/n} - Q$$

A combination of two or more Langmuir isotherms has been used as well, which implies two or more discrete affinities of adsorption (see tabel 2.1.1).

2 Properties of the phosphate adsorption

2.1 Adsorption isotherms

Numerous adsorption isotherms of phosphate on hydroxides, soils and sediments have been measured and reported. In this literature study no attempt has been made to produce a complete review of these measurements. Mainly conceptual features of phosphate adsorption are treated in the next paragraphs.
In this first section only some general descriptions are presented.

Olsen and Watanable (1957) discuss the use of Langmuir and Freundlich isotherms for adsorption of phosphate on clays and loams. They conclude that the Langmuir isotherm allows computation of the adsorption maximum. This maximum can be correlated with the surface area as determined by ethylene glycol (ethane - 1,2 diol) retention. The Langmuir isotherm is defined by

$$\frac{c}{(x/m)} = \frac{1}{Kb} + \frac{C}{b}$$

(See section 1.4.1, x/m is the amount (mg) P sorbed per 100 g soil).
The relationship between the maximum adsorption capacity b (mg P/100 g soil) and Et, the ethylene glycol retention (mg $(CH_2OH)_2$/g soil) was experimentally determined as:

$b = 0.276\ Et + 3.47$ (alkaline soils)

$b = 0.641\ Et + 5.7$ (acid soils)

Acid soils are, as can be expected, more reactive then alkaline soils. Olsen and Watanable give different values for the constant K (which is related to the Gibbs free energy of adsorption) for different soils:

$K = 1.4\ 10^4$ (1/mol) - Pierre Clay

$K = 1.0\ 10^4$ (1/mol) - Owyhee silt loam

F.A.M. de Haan (1965) measured the phosphate adsorption by a number of Dutch soils in the concentration range 0-200 mg P/1. The results are presented in

table 2.1.1. The Sticky soil and Oss soil have a higher iron content and accordingly a higher adsorption maximum.

Ryden, McLaughlin and Syers (1977C) used three Langmuir equations to describe phosphate sorption on iron oxide and one soil (see table 2.1.4; for the relation between ΔG and K see section 1.4.1). In a following article Ryden et al (1977B) give constants for some other soils (table 2.1.5).

McCallister and Logan (1978) compared the phosphate adsorption characteristics of soils and bottom sediments. The results are given in table 2.1.2. The adsorption capacity of sediments is much larger. This is possibly due to:

- preferential erosion of certain reactive size fractions of the whole soil, followed by some further concentration of this fraction by selective transport in the water body it self
- and/or chemical alternation of the eroded soil material after deposition in the stream.

Green, Logan and Smeck (1978) found correlations between phosphate adsorption parameters and calcite content of sediments (table 2.1.3). With increasing calcite content of the sediment studied the observed amount of phosphate in the sediments also increased whereas the adsorption energy decreased.

Although the phosphate is bound weakly by calcite, the precipitation of this mineral during algal growth may be an important mechanism controlling dissolved P-concentrations.

Lijklema and Hieltjes (1978) conclude that calcium carbonate may be an important conveyer of phosphate downward into the sediments, but that it plays a miner role in retaining the phosphate withing recently desposited sediments of eutrophic fresh water lakes.

2.2 Influence of ionic strength

In section 1.3 a quantitative model for phosphate adsorption has been presented. This model shows that at higher ionic strength the effects of the surface charge becomes less. Hence, if the surface is positively charged phosphate adsorption decreases with increasing concentration of indifferent ions, but if the surface is negativily charged, phosphate adsorption will increase with increasing ionic strength. Some experimental results related to this theory will be given here.

Helyar (1976A) measured phosphate adsorption on gibbsite in a large range of

phosphate concentrations (0.1 μ mol/1 - 1000 μ mol/1). The pH was 5.5 ± 0.1 (controlled by CO_2). Chloride salts of Ca^{2+}, Na^{+}, Mg^{2+}, K^{+} were added. The only anions present were HCO_3^- and Cl^-. According to Helyar the effect of HCO_3^- on adsorption was not measurable (see points 1 and 2 in fig. 2.2.1). Helyar and coworkers conclude from fig. 2.2.1:

1. Essentially the phosphate adsorption is not affected by Na^{+}, K^{+} or Mg^{2+}.
2. Ca^{2+} greatly increased P adsorption at equilibrium phosphate concentrations between 1 and 100 μ mol/1. This effect is not due to precipitation of calcite, calcium phosphate or hydroxy apatite. Obviously Ca^{2+} is strongly associated with the adsorbed phosphate groups, and in this way increases the adsorbing capacity.

According to Helyar (1976B) divalent cations with a radius near 1 Å will increase phosphate adsorption on Gibbsite. This is due to the lattice dimensions (see fig. 2.2.2). Thus Ca^{2+}, Cd^{2+} and Sr^{2+}, which increase adsorption, indeed have crystal-ionic radii of 0.99, 0.99 and 1.13 Å respectively.
Carrit and Goodgal (1954) measured phosphate adsorption by suspended sediments in seawater systems (fig. 2.2.3): Adsorption decreases with increasing salinity. Two explanations are given:

1. With increasing salinity the particles agglomerate and hence the surface area is reduced.
2. Sulphate is sorbed competitively.

Edzwald et al (1976) measured phosphate adsorption on kaolinite, montmorillonite and illite. His results are summarized in figure 2.2.4 A-C and table 2.2.1. The influence of ions as observed in this study conflicts with the results of Carrit and Goodgal (1954). Edzwald is of the opinion that the suspension of Carrit and Goodgal was aggregated, whereas in his experiments the suspensions was stirred vigerously.
Chen (1973B) discusses the effect of indifferent ions at higher pH values. The phosphate adsorption will increase due to cation adsorption resulting in a less negative surface charge. He measured phosphate adsorption α - Al_2O_3 and kaolinite in 0.01 mol/1 Na Cl solutions in presence of several other substances (see fig. 2.2.5 A-B) in order to evaluate the influence of polyvalent cations and anions. Indeed, the influence of polyvalent cations at high pH is substantial. (The adsorption of phosphate with 1.87 10^{-4} mol/1 Ca^{2+} addition at pH 12 is probably due to precipitation reactions). Anions are mainly ad-

sorbed on positively charged surfaces, and hence the greatest effects are observed in the acid region (fig. 2.2.5 C-D).
Particularly the influence of F^- is great: the radii of F^- and OH^- are about the same and hence F^- can replace the suface lattice hydroxyl ions. This decreases the phosphate adsorption.
Ryden (1977A) measured phosphate uptake by Egmont black loam and Porirua fine sandy loam. Calcium ions enlarged the phosphate adsorption especially at high phosphate surface coverage (negatively charged surface). According to Ryden the surface affinity ΔG and the capacity of the third Langmuir surface change (table 2.2.2).

2.3 Influence of silicate ions on phosphate adsorption

De Haan (1965) investigated the influence of silicate ions on phosphate adsorption on Na-montmorillonite. The phosphate uptake by the clay was measured after shaking 48 hours. Prior to equilibration the clay was treated with a Na_2SiO_3 solution (fig. 2.3.1). The phosphate adsorption by the clay is reduced significantly and the influence of pH decreases. The release of adsorbed phosphate due to silicate addition is a very fast process (fig. 2.3.2).
Obihara and Russel (1972) determined phosphate and silicate adsorption on soils. Figure 2.3.3 gives the envelope of the adsorption maximum as function of pH. At pH > 7 the adsorption maximum of phosphate is influenced by silicate adsorption. Figure 2.3.1 and 2.3.3 are not comparable, because De Haan used lower phosphate concentrations.
Bar-Yosef and Kafkafi (1978) measured phosphate desorption from kaolinite (by dialysis) in presence of dissolved SiO_2. They postulate the following two reactions:

$$x + P \rightarrow xP^* \qquad (1)$$

$$\{Si\} + xP^* \rightarrow xSi + \{P\} \qquad (2)$$

where

x = adsorption site
xP^* = activated complex
$\{\ \}$ = activity in solution

Reaction (2) is faster than (1) if sufficient SiO_2 is present. Hence the PO_4 desorption rate is proportional to xP. The experimental results of Bar-Yosef and Kafkafi are summarized in figure 2.3.4 in terms of the presented model. The activation energies are: 16.2 and 4.8 Kcal/mol for the fast and slow reaction respectively. Apparently the slow reaction is controlled by diffusion.
Brewster and coworkes (1975) found no influence of silicate on phosphate desorption at pH = 7 and a phosphate concentration of 0.04 mg P/1.

2.4 Kinetics of adsorption

Chen et al (1973B) measured PO_4 adsorption on alumina and kaolinite as a function of time, pH and temperature. At pH < 7 a distinction between a comparatively fast reaction, completed within 24 hours, and a slow reaction could be made.
This slow reaction continued for more then 40 days and was first order in phosphate concentration.
Table 2.4.1 summarizes the observed rate constants for the slow reaction. The rate strongly depens on pH. Doubling of the exposed surface area did not result in a concomittant doubling of the uptake rate. The effect of temperature on the rate was fairly small (E = 2.4 Kcal/mol).

The rate of the fast reaction, as evaluated from the measurements on the first day after addition, was proportional to the exposed surface. This indicates a proportionality between the number of available surface sites and the initial phosphate removal rate.
Also a new solid phase was formed: Al PO_4.n H_2O. This may explain the continuous slow reaction (under prevailing conditions of pH 4.3 and phosphate concentration 3.10^{-4} mol/1). However, addition of variscite as new cristallisation nuclei caused a decrease in the adsorption rate.
Kuo and Lotse (1972) measured the kinetics of phosphate adsorption on calcium carbonate and calcium kaolinite. The adsorption by calcium carbonate obeyed second-order kinetics, the rate being proportional to the available surface area and the phosphate concentration, according to:

$$\text{Phosphate} + \text{Surface} \underset{k_2}{\overset{k_1}{\rightleftharpoons}} \text{Product}$$

$$\frac{dx}{dt} = k_1 (C_o - x)(M - x) - k_2 x \qquad (4.1)$$

where

x = moles phosphate adsorbed/l

C_o = concentration of phosphate at t = 0 (mol/l)

M = concentration of adsorption sites at t = 0 (mol/l)

k_1, k_2 reaction rate constants

Integration of expression 4.1 results in:

$$\ln \left(\frac{x-A-B}{x+A-B}\right) = z\ A\ k_1 t + \ln \left(\frac{B+A}{B-A}\right) \qquad (4.2)$$

in which

$$A = \left[\frac{1}{4} \left(C_o + M + \frac{k_2}{k_1}\right)^2 - C_o M\right]^{1/4}$$

$$B = \frac{1}{2} \left(C_o + M + \frac{k_2}{k_1}\right)$$

Figure 2.4.1 shows a plot of the results of the measurements Kuo and Lotse; Table 2.4.2 gives the calculated rate constants (no value of k_2 was available). The second order rate constant k_1 decreases with increasing phophorus concentration in the $CaCO_3$ system. This is in accordance with Bronsted's theory, stating that the logarithm of the rate constant is inversly proportional to the square root of the ionic strength, when the reaction between two molecules involves charges of different sign. In contrast however, the rate constant for Ca-kaolinite-phosphate adsorption increases with increasing phosphate concentration.

In a following article Kuo and Lotse (1974A) describe the kinetics of phosphate adsorption by hematite and gibbsite. In this case a description in terms of an equation reminisent to the Freundlich isotherm has been used

$$x = K\ C_o\ t^{1/m} \qquad (4.3)$$

in which 1/m and K are constants, t is time, and x and C_o as defined previously, see equation 4.1.

The adsorption time t should not be too large, because the concentration c (see section 1.4.2.1) is considered to be constant.
The value of 1/m found was 0.08 for Gibbsite and 0.12 for hematite, independent of temperature and concentration (the pH has not been specified but was probably 7). Figure 2.4.2 shows the influence of the final phosphate concentration C (mg P/l) on the rate constant K. K is decreasing with increasing concentration (in accordance with Bronsted's theory). The effect of temperature was small (E = 1.9 kcal/mol, based on 3-4 measurements between 5 and 40°C).
Other experiments by Kuo and Lotse (1974B) with 2 washed lake sediments showed that 1/m was 0.182 for both sediments (see table 2.4.3 for sediment composition). Again the effect of temperature was small: E = 2.74 kcal/mol (4-40°C). The rate constents K found were 0.2 (sediment 14) and 0.4 (sediment 12).
Barrow and Shaw (1975A) use a slightly different formulation for the kinetics of adsorption.
They define two consecutive processes

$$A \overset{\rightarrow}{\leftarrow} B \overset{\rightarrow}{\leftarrow} C$$

A = phosphate in solution
B = phosphate, adsorbed and in direct contact with the solution
C = phophate that is no longer in direct contact with the phosphate in solution.

Barrow and Shaw propose the following rate equation for the transfer from B → C:

$$\frac{d\alpha}{dt} = k(1-\alpha)^n \qquad (4.4)$$

in which k and n are constants and α is the fraction of phosphate transferred from B to C.
With the initial condition t = 0, α = 0 (4.4) can be integrated into:

$$1 - \alpha = [(n-1)\ kt + 1]^{1/(n-1)} \qquad (4.5)$$

For large kt this can be simplified into

$$1 - \alpha = (kt/b_1)^{-b_1} \qquad (4.6)$$

with

$$b_1 = 1/(n-1)$$

If B_o and B_t are the concentrations of phosphate in the form B at t = 0 and t = t, then:

$$B_t = B_o(kt/b_1)^{-b_1} \qquad (4.7)$$

According to Barrow and Shaw the Freundlich isotherm is applicable to non calcareous sediments at low phosphate content:

$$B_t = aA_t^{b_2} \qquad (4.8)$$

A_t = phosphate concentration in solution
a, b_2 = constants

Combination of 4.7 and 4.8 yields

$$A_t^{b_2} = (B_o/a)(kt/b_1)^{-b_1} \qquad (4.9)$$

B_o is unknown, but if the solution/soil ratio is low enough and not too much phosphate is added, most of the dissolved phosphate will be adsorbed, and B_o will be proportional to the amount of phosphate added:

$$B_o = m\ P \qquad (4.10)$$

m = proportional constant
P = amount Padded (mg P/1)

The rate constant k is affected by the temperature in accordance with the Arrhenius equation:

$$k = k_o \exp(-E/RT) \qquad (4.11)$$

Substitution of 4.10 in 4.11 gives

$$\ln A_t = K_1 + K_2 \ln P - K_3 \ln t + K_4/T \qquad (4.12)$$

in which

$K_1 = 1/b_2 \ln(m/a) - b_1/b_2 \ln(k_o/b_1)$

$K_2 = 1/b_2$

$K_3 = b_1/b_2$

$K_4 = b_1E/(b_2R)$

Results of measurements with 17 soils from South West Australia are presented in tables 2.4.4 A and B.
The apparent activation energy is much higher than found by Kuo and Lotse (1974A,B). This is due to the different formulations used for k in 4.6 and K in 4.3 resulting in difference by a factor 1/m in the activation energies.

2.5 Desorption isotherms

Medina and López-Hernandez (1978) used different methods to extract adsorbed phosphate from Venezuelan soils. Some of their results are given in figure 2.5.1. Specific adsorbing ions (citrate) release more phosphate than agents that only lower the ambient phosphate concentration such as resins. The effect of higher ionic strength, a reduction of the interaction between the positive charged surface (pH = 4) and the phosphate, is comparatively small.
J.M. Andersen (1975) measured phosphate desorption from eutrophic-lake sediments at different pH values. 80% of the water above the sediments was replaced every four or five days by lake water and the pH was adjusted. The phosphate concentration in the lake water was 0.2 mg P/l. Figures 2.5.2 A and B show the results of his work. The rate of the phosphate release increases with increasing pH. At pH > 9.5 the rate decreases, calcium behaves similary. Anderson supposes that this is due to precipitation of apatite or by co-precipitation of $CaCO_3$.

Barrow and Shaw (1979A) investigated the influence of indifferent ions on phosphate desorption from a soil. The soil was incubated with 1 mg P/g Soil (added as $CaHPO_4$). Desorption was induced by dilution. Figure 2.5.3.A is an example of the results. Phosphate desorption decreases with increasing calcium concentration. Barrow and Shaw used the following empirical formulation for the description of phosphate desorption:

$$P_d = K_p t_d^m - a_2 t_d^n c^b = cS \qquad (5.1)$$

where

P_d = phosphate desorbed (µg P/g soil)
t_d = period of desorption (h)
c = solution concentration (µg P/ml)
S = solution soil ration (ml/g soil) desorption by dilution
K_p, m, n, a_2 = constants

Values of the constants are given in table 2.5.1. The figures 2.5.3 B and C show the influence of different monovalent cations on phosphate and calcium desorption. Larger ions displace more calcium while less phosphate is desorbed. This is in contradiction with the specific calcium surface complex postulated by Helyar et al (1976ß, see section 2.2), but consistent with the results of Ryden and Syers (1976) who found that calcium can be replaced by potassium without releasing all the adsorbed phosphate. Barrow and Shaw emphasize that an electrostatical interpretation (for instance Bowden (1977), see section 2.3) should be used. Larger cations differ in hydration energy and polarizability from small cations and will be adsorbed in the Stern layer. This increases the surface charge, so that the phosphate remains adsorbed.
In a subsequent article of Barrow (1979) phosphate desorption has been described as a proces limited by two factors:

- P_o; representing the amount of P that will be desorbed at zero phosphate concentration and
- C_e; representing the solution concentration at which no net desorption occurs.

$$P_o = a\, C_e^{b_1} \qquad \text{(Freundlich)} \quad (5.2)$$

$$P_d = a(C_e^{b_1} - C^{b_1}) = CS \qquad (5.3)$$

where

P_d = amount phosphate desorbed μg P/g soil

S = soil/solution ratio ml/g

a, b_1 = constants

b_1 is about 0.4, and using

$$a = a_2 t_d^{b_2} \qquad (5.4)$$

$$C_e^{b_1} = C_{e,o}^{b_1}(1+k\ t_d)^{-b_3} \qquad (5.5)$$

where

t_d = desorption time (h)

$C_{e,o}$ = initial equilibrium phosphate concentration (mg P/l) = C_e at $t_d = 0$

k = kinetic constant

we have a set of equations describing the phosphate desorption by dilution. Barrow used for his experiments a Dardanup clay loam with a large phosphate adsorption capacity; extracted iron and aluminium were 2.9 and 0.7% respectively. The soil was incubated at different temperature, during selected times and at various concentrations of calcium dihydrogen phosphate in 0.01 M calcium chloride. Desorption was measured by increasing the solution/soil ratio (dilution).

From table 2.5.3 and figure 2.5.4 we can see the influence of the incubation time on desorption:

$$\ln C_{e,o}^{b_1} = 0.786 - 0.247 \ln t_i \qquad (5.6)$$

in which

t_i = incubation time (days at 25°C)

Both the initial equilibrium phosphate concentration $C_{e,o}$ and the rate constant k decrease with increasing incubation time and temperature (table 2.5.3). At short incubation times the phosphate release is fast followed by a subsequent slow adsorption (see fig. 2.5.5.B/C). Barrow Shaw (1975 C) found a

similar effect, which was caused by disintegration of the particles: the exposed surface area increased by shaking. (This was certainly not the case in their 1979 experiments). Using the equation

$$A_t = \left[\frac{k_3 t_d^{b_2} t_i^{-b_3} P_i - P_d}{k_1 t_d^{b_2}} \right]^{1/b_1} \qquad (5.7)$$

with

A_t = phosphate concentration in solution (mg P/l)
k_3, k_1 = rate constants
t_d = time of desorption (h)
t_i = time of incubation
P_i = amount of phosphate adsorbed during the incubation (µg P/g soil)
P_d = amount of phosphate desorberd (µg P/g soil)
b_1, b_2, b_3 = constants

Barrow and Shaw (1975C) found for the yellowish brown loam described in figure 2.5.3.A:

$$k_1 = 41.7,\ k_3 = 0.102,\ b_2 = 0.298,\ b_3 = 0.253$$

b_1 was taken 0.406.
Figure 2.5.7 shows some of their results.
The influence of aging on phosphate adsorption has also been discussed by Kuo and Lotse (1974B). Only a small fraction (0.15%) of native adsorbed phosphate in sediments desorbed with F^- and OH^- extration. With freshly adsorbed phosphate the degree of desorption was higher (compare fig. 2.5.6.A and B).
Ryden and Syers (1977D) also found a decreasing desorption capacity upon aging, see figure 2.5.8. They concluded that physically bound phosphate is converted into chemically bound phosphate.
Brewster and coworkers (1975) applied both dilution a desorption by addition of a resin at pH about 7 on loamy sandy soils. A description according to the Freundlich isotherm showed differences in the obtained values for the constants, see table 2.5.4 and figure 2.5.9. This is probably due to differences in pH, if the phosphate concentrations were expressed in mono calcium phos-

phate potentials by taking into account the calcium phosphate complex ion formation, both technique gave similar results:

resin $\quad (\frac{1}{2}\ p\ Ca + p\ H_2PO_4) = 5.71 + 0.064\ \Delta P$

dilution $(\frac{1}{2}\ p\ Ca + p\ H_2PO_4) = 5.95 + 0.061\ \Delta P$

(ΔP in 10^{-7} mol P/g ovendry soil).

2.6 The influence of pH on phosphate sorption

Huang (1975) summarized the influence of pH on the adsorption capacity and adsorption affinity of some alluminum (hydr)oxides. He used the Langmuir isotherm:

$$1/x = 1/(K_{ads} b[c]) + 1/b \qquad (6.1)$$

Where:

- x = amount of phosphate sorbed
- K_{ads} = energetic constant
- b = adsorption capacity
- c = phosphate concentration in the solution

The maximum adsorption capacity b and the energetic constant K_{ads} are strongly dependent on pH (see table 2.6.1). Based on an adsorption model with the chemical potential of the ions in the solution as the sole independent variable (analogous to Hingston et al, 1972) Cabrera and coworkers (1977) described the adsorption maximum b for several oxides as:

$$b = [RT \ln \alpha(1-\alpha) + \mu^\circ_{total}\}]\ C_1 \qquad (6.2)$$

in which

$$\mu^\circ_{total} = \mu^\circ_{H_3PO_4} + \mu^\circ_{H_2PO_4^-} + \mu^\circ_{H\ PO_4^=} + \mu^\circ_{PO_4^\equiv}$$

α = degree of dissociation

$$= \frac{K_1[H^+]^2 + K_1K_2[H^+] + K_1K_2K_3}{[H^+]^3 + K_1[H^+]^2 + K_1K_2[H^+] + K_1K_2K_3}$$

and K_1, K_2, K_3 the dissociation constants of H_3PO_4.
The parameter C_1 is a function of the chemical affinity of the ion for the oxide and of the surface area. Values of C_1 and μ°_{total} are given in table 2.6.2. According to equation 6.2 adsorption will decrease continuously with increasing pH.

However, Breeuwsma and Lyklema (1973) found with hematite at higer phosphate concentrations humps in the pH dependency of phosphate adsorption (fig. 2.6.1). At lower phosphate concentrations the effect disappears.
Carrit (1954) used suspended river mud as adsorbent. Maximum adsorption occurred at a pH of about 5 (fig. 2.6.2).
Effects of silications and of other ions on the pH influence have been discussed in section 2.2 and 2.3.

2.7 Influence of the redoxpotential on phosphate sorption

O.S. Jacobsen (1977, 1978) investigated phosphate sorption on well mixed lake sediments (fig. 2.7.1). Note that in iron rich sediments the sorption at low redox potential is less than in oxidezed sediments. In case of calcareous sediments this effect was less, cf. line I and II of Esröm Sö. Jacobsen (1978) suggest that reduction of the sediments may cause a reduction in the number of active iron sites. Under such conditions and also at high pH the phosphate concentration will increase and apatite formation might occur.
Using mud-water systems treated with antibiotics Hayes and Philips (1958) demonstrated through P^{32} tracer techniques, that the amount of P^{32} adsorbed by oxidized mud is larger then the amount of P^{32} adsorbed by reduced mud (see fig. 2.7.2). Without application of antibiotics to kill the micro organisms the difference was insignificant.
Patric and Kahlid (1974) varied the phosphate concentration and the redox potential in soil suspensions. At low phosphate concentrations (no P-added) oxidised soils adsorbed more than reduced soils. At higher phosphate concen-

trations this effect was reversed (fig. 2.7.3). The authors concluded that under reduced circumstances highly dispersed ferrous forms increase the activity and the surface area of the iron compounds reacting with phosphate. The quantity of iron and the concomittant phosphate extracted under anaerobic conditions by oxalate was higher than with oxidised soils. Oxalate is believed to dissolve amorphous and poorly crystallized Fe oxides.
The binding on ferric oxides is stronger, but the exposed surface area is smaller.
Halford and Patric (1979) tried to discriminate between the effects of reduction and of pH changes on phosphate sorption. They used a silt loam containing 0.3% rice straw. The soil was incubated during 25 days at 30°C, the redox potential was decreased by addition of a nitrogen source and dextrose (microbiological oxidation). The redox potential was controlled by the amount of air added during the incubation. For the mathematical description they used a two surface Langmuir isotherm:

$$x = k'x'_m\, C/(1+k'C) + k''x''_m\, C/(1+k''C) \qquad (7.1)$$

in which

C = final solution concentration of phosphate
x = amount of phosphate adsorbed
k = equilibrium constant related to the bonding energy
x_m = maximum adsorption capacity

The subscripts ' and " refer to the high and low energy surfaces respectively. The phosphate buffer capacity (the maximum of the slope of the adsorption isotherm) is defined by

$$\left(\frac{dx}{dc}\right)_{c\to 0} = k'x'_m + k''x''_m \qquad (7.2)$$

The results of their measurements are given in tables 2.7.3.A-C and figures 2.7.4.A-C. At pH = 8 both the fraction of labil P and the adsorption capacity increase, but upon reduction the adsorption energy decreases. The Fe concentration in the solution increases by reduction, especially at low pH. The increase of the adsorption capacity can be explained by $Fe_3(PO_4)_2$ precipitation. This is shown in figure 2.7.4.A. At pH = 8 the adsorption is also influenced by calcium phosphate precipitation, the Ca^{2+} concentration was about

0.01 M.

In reduced soils the phosphate adsorption increases with increasing pH. Jørgen, Kamp-Nielsen and Jacobsen (1975) and Kamp-Nielsen (1975) presented models for sediment-water exchange. The models were calibrated with experimental data from eutrophic lakes. Below 17°C the phosphate release rate was higher for reduced sediments.

2.8 Irreversible reactions

Lijklema (1980) investigated the interaction of O-phosphate with (amorphous) iron (III) and aluminum hydroxides. Figure 2.8.1 shows that the adsorption/desorption reactions due to changes in pH are not reversible within one day. Also there is a difference in adsorption capacity between freshly precipitated hydroxide and a one day old precipitate (fig. 2.8.2): the structure of the adsorbent changes.

The effect of longer adsorption times can be seen from figure 2.8.3 (Carrit, 1954). After a long adsorption time a smaller fraction of the adsorbed phosphate is released quickly upon desorption. This can be due to diffusion of phosphate into the soil particles and/or slow precipitation reactions.

Barrow and Shaw (1975C) measured the influence of incubation time on phosphate desorption from soils (see also 2.5). Evidently the amount of reversibly sorbed phosphate decreases at enhanced incubation times (fig. 2.8.4).

Hingston, Posner and Quik (1974) investigated the reversibility of phosphate adsorption on goethite and gibbsite. They defined:

$$\text{desorbability} = \frac{\text{original adsorption} - \text{adsorption after 2 washes}}{\text{original adsorption} - \text{calculated adsorption}^{1)}} * 100\%$$

The original adsorption was obtained after 1 day equilibrium at 20°C. Only the phosphate concentration in the solution was changed: pH and ionic strength were constant. Figure 2.8.5 A, B present their results. At low ionic strength the desorbability is decreasing with decreasing initial adsorption. At low initial phosphate adsorption the adsorption is essentially irreverisble. This

1) Calculated from the adsorption isotherm at the solution concentrations after two washes = amount phosphate adsorbed in case of reversible reactions. Complete reversible adsorption gives the desorbability a value of 100%, while irreversible adsorption gives a value of zero.

is possibly due to the high positive surface charge at low surface coverage. At high ionic strength the effects of charge are less (see also section 1.3) and the desorbability becomes quite independent of surface coverage (e.g. pH = 9, 1 M Na Cl). At pH = 4.5 the desorbability is very low due to the positive suface charge. The desorbability from goethite is significantly lower than from gibbsite, but the influence of ionic strength is similar to that of gibbsite.

At low phosphate concentrations adsorption becomes reversible only with long equilibration times (White and Taylor, 1977). Probably their opinion is that small extra additions of phosphate will be adsorbed reversibly. The high energy sites on the surface will be occupied at low phosphate concentration and long equilibration times. Hence with additional phosphate only low energy sites are available and adsorption is therefore reversible. If the equilibration time is short, there is a chance that not all high energy are occupied. Hence, a part of the additional phosphate (marked by ^{32}P) will be irreversibly adsorbed.

The results of Hingston, Posner and Quick (1974) are explained by the fact that the initial phosphate concentration must have been very high (> 1 m M). This can be inferred from the high adsorption capacity on gibbsite and hematite and the soil/solution ratio used. At these high phosphate concentrations also precipitation reactions can take place, resulting in irreversibly precipitated phosphates.

Barrow and Shaw (1975B) measured the influence of time and temperature on the decrease of isotopically exchangeable phosphate. They found for a yellowish-brown loamy sand:

$$\ln(P_e) = \ln P - b_1 \ln(A \exp(-E/RT)\ t/b_1 + 1) + b_2 \qquad (8.3)$$

In which:

P_e = amount of soil phosphate exchanged
= P^{31} (solution) * $(P_o^{32}-P_t^{32})/P^{32}$ where P_o^{32} and P_t^{32} are respectively the initial and final amounts P^{32} in solution

P = quantity phosphate added (µg P/g soil)

T = temperature of incubation (°K)

t = period of incubation (days)

t_e = period of equilibration (days)

A = coefficient: $2.46\ 10^{16}$ day^{-1}

E = apparent activation energy 23.6 kcal/mole

b_1 = constant, 0.288

b_2 = constant, 0.342

A longer incubation time and a higher temperature reduce the isotopic exchange rate. It has been suggested that this is due to conversion of a part of the phosphate into non exchangeable forms. Equation 8.3 is not valid for high values of t_e ($\ln P_e/P$ must be negative, see fig. 2.8.6, lined).

LITERATURE

ANDERSEN, J.M. (1975), "Influence of pH on release of phosphorus from lake sediments",
Arch. Hydrobiol. 76 (4) 411-419.

ANDERSON, M.A. and MALOTKY D.T. (1979), "The adsorption of protolyzable anions on hydrous oxides at iso-electric pH",
J. of Coll. Interface Sci. 72 413-427.

ATKINSON, R.J., POSNER, A.M. and QUIRK, J.P. (1972), "Kinetics of isotopic exchange of phosphate at the α FeOOH-aqueous solution interface",
J. Anorg. nucl. Chem. 34 2201-2211.

BARROW, N.J. and SHAW, T.C. (1975A), "The slow reactions between soil and anions: 2. Effect of time and temperature on the decrease in phosphate concentration in he soil solution",
Soil Sci. 119 167-177.

BARROW, N.J. and SHAW, T.C. (1975B), "The slow reactions between soil and anions: 3. The effects of time and temperature on the decrease in isotopically exchangeable phosphate",
Soil Sci. 119 190-197.

BARROW, N.J. and SHAW, T.C. (1975C), "The slow reactions between soil and anions: 5. Effects of period of prior contact on desorption of phosphate from soils",
Soil Sci. 119 311-320.

BARROW, N.J., (1979), "The description of desorption of phosphate from soil",
J. of Soil Sci. 30 259-270.

BARROW, N.J. and SHAW, T.C. (1979A), "Effects of ionic strength and nature of the cation on desorption of phosphate from soil",
J. of Soil Sci. 30 53-65.

LITERATURE (continued)

BARROW, N.J. and SHAW, T.C. (1979B), "Effects of solution: soil ratio and vigour of shaking on the rate of phosphate adsorption by soil",
J. of Soil Sci. 30 67-76.

BAR-YOSEF, B. and KAFKAFI, U. (1978), "Phosphate desorption from kaolinite suspensions",
Soil Sci. Soc. of Am, J. 42 570-574.

BEEK, J. and RIEMSDIJK, W.H. VAN (1979), "Interaction of orthophosphate ions in soil",
in: Soil Chemistry part B: Physico Chemical Models, Developments in Soil Science 5B p. 259-284, ed. G.H. Bolt, Elsevier.

BOWDEN, J.W., BOLLAND, M.D.A., POSNER, A.M. and QUIRK, J.P. (1973), "Generalized model for anion and cation adsorption at oxide surfaces",
Nature Physical Science 245 81-83.

BOWDEN, J.W., POSNER, A.M. and QUIRK, J.P. (1977), "Ionic Adsorption on variable charge mineral surfaces. Theoratical - charge development and titration curves",
Aust. J. Soil Res. 15 121-136.

BREEUWSMA, A. (1973), "Adsorption of ions on hematite (α - Fe_2O_3)",
These IV Dissertation, Agricultural University, Wageningen, The Netherlands (Thesis in Dutch).

BREEUWSMA, A. and LYKLEMA, J. (1973), "Physical and chemical adsorption of ions in the electrical double layer on hematite (α - Fe_2O_3)",
J. of Coll. and Interface Sci. 43 437-448.

BREWSTER, J.L., CANCHEVA, A.N. and NYE, P.H. (1975), "The determination of desorption isotherms for soil phosphate using low volumes of solution and an anion resin",
J. Soil Sci. 26 364-377.

LITERATURE (continued)

BRINKMAN, A.G. (1979), "Adsorptie van ionen aan geladen kolloidale deeltjes", Internal Report, Twente University of Technology, department of chemical technology, report number CT79/095/1311.

CABRERA, F., MADRID, L. and ARAMBARRI, P. DE (1977), "Adsorption of phosphate by various oxides: Theoretical treatment of the adsorption envelope", J. of Soil Sci. 28 306-313.

CARRIT, D.E. and GOODGAL, S. (1954), "Sorption reactions and some ecological implications", Deep Sea Research 1 224-243.

CHEN, Y.S.R., BUTLER, J.N. and STUMM, W. (1973A), "Kinetic Study of phosphate reaction with aluminum oxide and kaolinite", Env. Sci. Techn. 7 327-332.

CHEN, Y.S.R., BUTLER, J.N. and STUMM, W. (1973B), "Adsorption of phosphate on alumina and kaolinite from dilute aqueous solutions", J. Colloïd and Interface Sci. 43 421-436.

EDZWALD, J.K., TOENSING, D.C. and CHI-YEW LEUNG, M. (1976), "Phosphate adsorption reactions with clay minerals", Env. Sci. techn. 10 485-490.

GREEN, D.B., LOGAN, T.J. and SMECK, N.E. (1978), "Phosphate adsorption-desorption characteristics of suspended sediments in the Maumee River Basin of Ohio", J. Env. Qual. 7 208-212.

HAAN, F.A.M. DE (1965), "The interaction of certain inorganic anions with clays and soils", Thesis, Agricultural University, Wageningen, The Netherlands; Centre for Agricultural Publishing and Documentation, Agric. Res. Report 655.

LITERATURE (continued)

HAYES, F.R. and PHILLIPS, J.E. (1958), "Lake water and sediment: IV Radio phosphorus equilibrium with mud, plants and bacteria under oxidized and reduced conditions",
Limn. Ocean. 3 459-475.

HELYAR, K.R., MUNNS, D.N. and BURAU, R.G. (1976A), "Adsorption of phosphate by gibbsite 1. Effects of neutral chloride salts of calcium, magnesium, sodium and potassium",
J. of Soil Sci. 27 307-314.

HELYAR, K.R., MUNNS, D.N. and BURAU, R.G. (1976B), "Adsorption of phosphate by gibbsite 2. Formation of a suface complex involving divalent cations",
J. of Soil Sci. 27 315-323.

HINGSTON, F.J., POSNER, A.M. and QUIRK, J.P. (1972) "Anion adsorption by goethite and gibbsite I. The role of the proton in determining adsorption envelopes ",
J. of Soil Sci. 23 177-192.

HINGSTON, F.J., POSNER, A.M. and QUIRK, J.P. (1974), "Anion adsorption by goethite and gibbsite II. Desorption of anions from hydrous oxide surface",
J. of Soil Sci. 25 16-26.

HOLFERD, I.C.R. and PATTRIK Jr., W.H. (1979), "Effects of reduction and pH changes on phosphate sorption and mobility in an acid soil",
Soil Sci. Soc. Am., J. 43 292-297.

HUANG, C.P. (1975), "Adsorption of phosphate at the hydrous γ-Al_2O_3. Electrolyte Interface",
J. of Coll. and interface Sci. 53 178-186.

JACOBSEN, O.S. (1977), "Sorption of phosphate by Danish Lake Sediments",
Vatten 3 290-298.

LITERATURE (continued)

JACOBSEN, O.S. (1978), "Sorption, adsorption, chemosorption of phosphate by Danish lake sediments",
Vatten 4 230-242.

JØRGENSEN, S.E., KAMP-NIELSEN, L. and JACOBSEN, O.S. (1975), "A submodel for anaerobic mud-water exchange of phosphate",
Ecol. Mod. 1 133-146.

KAMP-NIELSEN, L. (1975), "A kinetic approach to the aerobic sediment-water exchange of phosphorus in Lake Esrom",
Ecol. Mod. 1 153-160.

KAFKAFI, U., POSNER, A.M. and QUIRK, J.P. (1967),
Soil Sci. Soc. Am., Proc. 31 348-353 cited by Rayan (1975).

KITTRICK, J.A. and JACKSON, M.L. (1956), "Electron-microscope observations of the reaction of phosphate with minerals leading to an unified theory of phosphate fixation in soils",
J. of Soil Sci. 7 81-89.

KUO, S. and LOTSE, E.G. (1972), "Kinetics of phosphate adsorption by calcium carbonate and Ca-kaolinite",
Soil Sci. Soc. Am. Proc. 36 725-729.

KUO, S. and LOTSE, E.G. (1974A), "Kinetics of phosphate adsorption and desorption by hematite and gibbsite",
Soil Sci. 116 400-406.

KUO, S. and LOTSE, E.G. (1974B), "Kinetics of phosphate adsorption and desorption by lake sediments",
Soil Sci. Soc. of Am., Proc. 38 50-54.

LEVINE, S., MINGINS, J. and BELL, G.M., "The discrete-ion effect in the ionic double layer theory" (Review),
J. Electro anal. Chem. 13 (1967) 280-329.

LITERATURE (continued)

LEVINE, S. and SMITH, A.L. (1971), "Theory of the differential capacity of the oxide/aqueous electrolyte interface",
Disc. Faraday Soc. 52 290-301.

LIJKLEMA, L. (1980), "Interaction of O-phosphate with iron (III) and aluminum hydroxides",
Env. Sci. Techn. 14 537-541.

LIJKLEMA, L. and HIELTJES, A.H.M. (1978), "On the role of iron and calcium in the cycling of phosphate in shallow lakes",
Paper presented at the Workshop on Hydrophysical and ecological models for shallow lakes and reservoirs held at the International Institute for Applied Systems Analyses 11-14 April 1978 Luxemburg Austria.

McCALLISTER, D.C. and LOGAN, T.J. (1978), "Phosphate adsorption-desorption characteristics of soils and bottom sediments in the Maumee river basin of Ohio",
J. Env. Qual. 7 87-92.

MEDINA, A. and LOPEZ-HERNANDEZ, D. (1978), "Method of desorbing soil phosphate for application to P description isotherm construction",
Trop. Agric. (Trinidad) 55 69-76.

MULJADI, D., POSNER, A.M. and QUIRK, J.P. (1966), "The mechanism of phosphate adsorption of kaolinite, gibbsite and pseudo boehmite",
J. Soil Sci. 17 212-228.

NRIAGU, J.O. (1972), "Stability of vivianite and ion-pair formation in the system $Fe_3(PO_4)_2$ - H_3PO_4 - H_2O",
Geochimica et Cosmchimica Acta 36 459-470.

NRIAGU, J.O. (1976), "Phosphate - Clay mineral relations in soils and sediments",
Can. J. of Earth Sci. 13 717-736.

LITERATURE (continued)

OBIHARA, C.H. and RUSSELL, E.W. (1972), "Specific adsorption of silicate and phosphate by soils",
J. of Soil Sci. 23 105-117.

OLSEN, S.R. and WATANABE, F.S. (1957), "A method to determine a phosphorus adsorption maximum of soils as measured by the Langmuir isotherm",
Soil Sci. Soc. Proc. 21 144-149.

OVERBEEK, J.TH.G. (1952)
in: Colloid Science Vol. I p. 130
ed H.R. Kruyt, Elzevier 1952.

PARFITT, R.L., ATKINSON, R.J. and SMART R.ST.C. (1975), "The mechanism of phosphate fixation by iron oxides",
Soil Sci. Soc. Am, Proc. 39 837-841.

PARFITT, R.L. (1977), "Phosphate adsorption on an oxisol",
Soil Sci. Soc. Am., J. 41 1064-1067.

PARFITT, R.L. (1979), "The nature of the phosphate goethite (α FeOOH) complex formed with $Ca(H_2PO_4)_2$ at different surface coverage",
Soil Sci. Soc. Am., J. 43 623-625.

PATRICK, W.H. Jr. and KAHLID (1974), "Phosphate release and sorption by soils and sediments. Effect of aerobic and anaerobic conditions",
Science 186 53-55.

PONEC, V., KNOR, Z. and CERNY, S., "Adsorption on Solids",
page 352, Butterworth Group, London 1974.

RAYAN, S.S.S., PERROTT, K.W. and SAUNDERS W.M.H. (1974), "Identification of phosphate-reactive sites of hydrous alumina from proton consumption during phosphate adsorption at constant pH values",
J. Soil Sci. 25 438-447.

LITERATURE (continued)

RAYAN, S.S.S. (1975), "Adsorption of divalent phosphate on hydrous aluminium oxide",
Nature 253 434-436.

RIEMSDIJK, W.H. VAN (1979), "Reaction mechanisms of phosphate with $Al(OH)_3$ and a sandy soil",
Thesis, Agricultural University Wageningen, The Netherlands.

RYDEN, J.C. and SYERS, J.K. (1976), "Calcium retention in response to phosphate sorption by soils",
Soil Sci. Soc. Am. J. 40 845-846 (cited by Barrow (1979)).

RYDEN, J.C., SYERS, J.K. and McLAUGHLING, J.R. (1977A), "Effects of Ionic Strength on chemosorption and potential-determing sorption of phosphate by soils",
J. Soil Sci. 28 62-71.

RYDEN, J.C., SYERS, J.K. and McLAUGHLING, J.R. (1977B), "Mechanisms of phosphate sorption by soils and hydrous ferric oxide gel"
J. of Soil Sci. 28 72-92.

RYDEN, J.C., McLAUGHLING, J.R. and SYERS, J.K. (1977C), "Time-dependent sorption of phosphate by soils and hydrous ferric oxides",
J. Soil Sci. 28 585-595.

RYDEN, J.C. and SYERS, J.K. (1977D), "Desorption and isotopic exchange relationships of phosphate sorbed by soils and hydrous ferric oxide gel",
J. Soil Sci. 28 596-609.

STERN, O. (1924), "On the theory of the electrical double layer",
Z. Electrochem. 30 508 cited by Bowden cs. (1977).

STUMM, W. and SIGG, L. (1979), "Kolloïd chemische Grundlagen der Phosphor-Elimination in Fällung, Flockung und Filtration",
Z.f. Wasser- und Abwasser Forschung 12 37-47.

LITERATURE (continued)

WHITE, R.E. and TAYLOR, A.W. (1977), "Reactions of soluble phosphate with acid soils: the interpretation of the adsorption-desorption isotherms", J. of Soil Sci. 28 314-318.

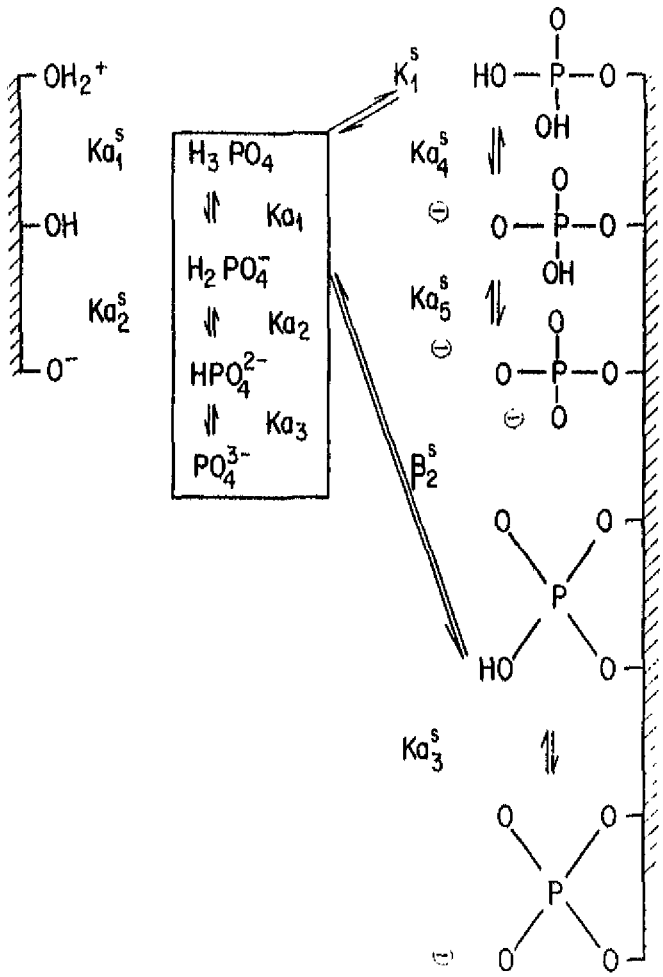

: Wechselwirkungen der Oxidoberfläche mit H⁺, OH und Phosphat

Die chemische Wechselwirkung der Oberfläche eines Oxids oder Oxidhydroxids von Fe(III) mit Phosphat. Ähnliche Reak

Scheme 1.1 From Sigg and Stumm (1979)

Gleichgewichtsreaktionen für die Bindung von Phosphat an α-FeOOH- Oberflächen

	log K_{intr}
$\equiv FeOH_2^+ \rightleftarrows \equiv FeOH + H^+$	Ka_1^s - 6,4
$\equiv FeOH \rightleftarrows FeO^- + H^+$	Ka_2^s - 9,25
$\equiv FeOH + H_3PO_4 \rightleftarrows \equiv FePO_4H_2 + H_2O$	K_1^s - 9,5
$\equiv FePO_4H_2 \rightleftarrows \equiv FePO_4H^- + H^+$	Ka_4^s - 4,4
$\equiv FePO_4H^- \rightleftarrows \equiv FePO_4^{2-} + H^+$	Ka_5^s - 6,6
$2 \equiv FeOH + H_3PO_4 \rightleftarrows \equiv Fe_2PO_4H + 2H_2O$	β_2^s 8,5
$\equiv Fe_2PO_4H \rightleftarrows \equiv Fe_2PO_4^- + H^+$	Ka_3^s - 4,0

Table 1.1

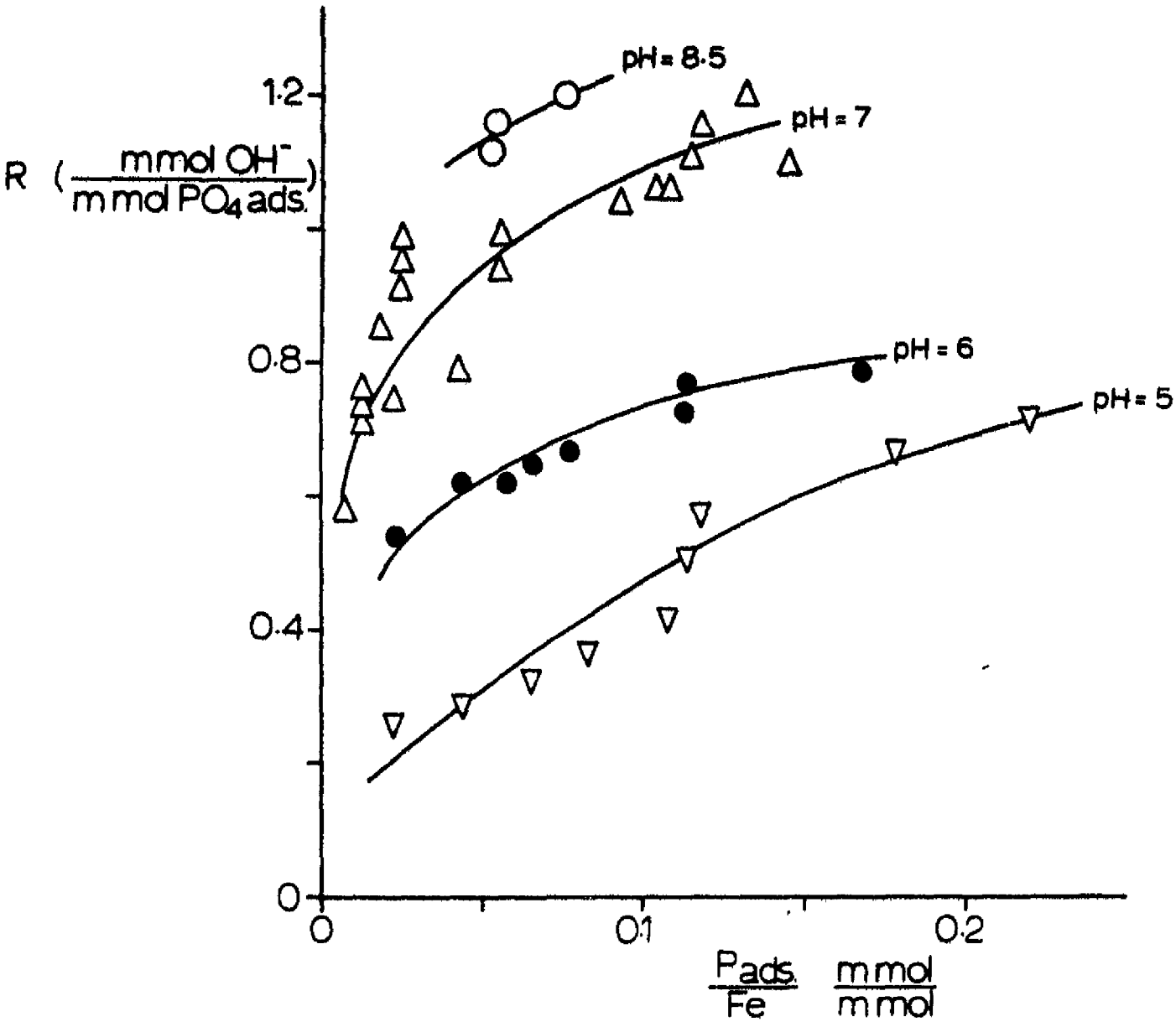

Figure 1.1 R as function of pH and extent of adsorption

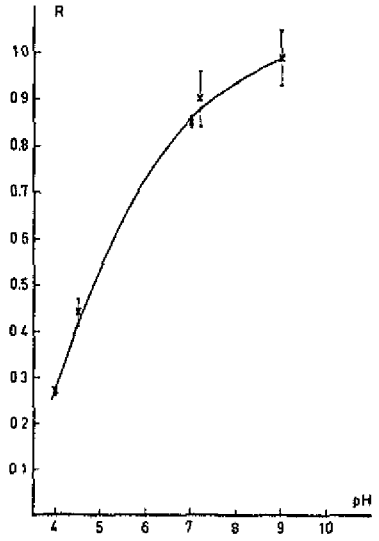

Ratio R in mole/mole of the amount of acid (required to keep pH constant during the adsorption of phosphate on hematite) and the amount of phosphate adsorbed.

Figure 1.2

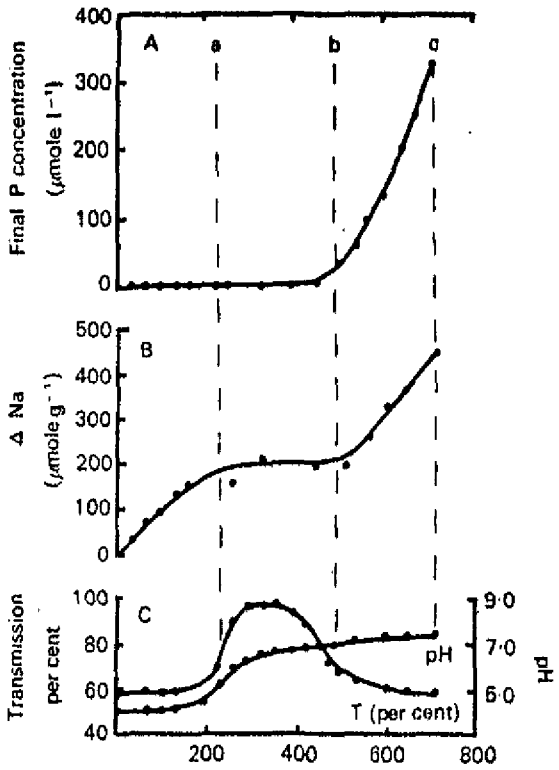

Added P sorbed μ mol/g

Isotherm for the sorption of P by Fe gel; B, the relationship between the difference (ΔNa) in the Na uptake by Fe gel in the presence and absence of added P for the same addition of Na, and the amount of added P sorbed; C, the relationship between the transmission (%T) and pH of Fe gel suspensions, and the amount of added P sorbed

Figure 1.3

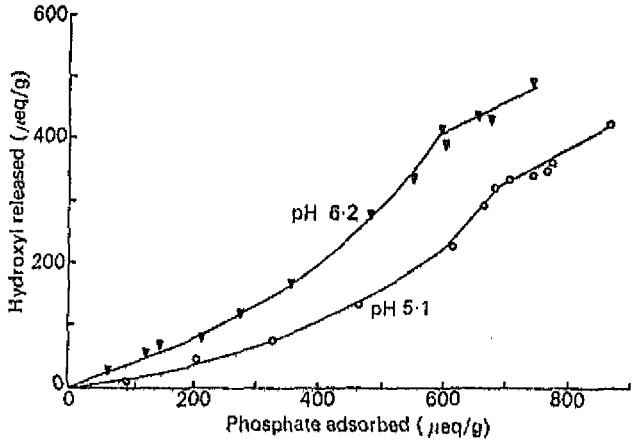

Amounts of hydroxyl ions released from hydrous alumina during phosphate adsorption plotted as a function of phosphate adsorbed. The plot of pH 5·1 represents equations 5 and 7 and that of pH 6·2 represents equations 6 and 8.

Figure 1.4.A

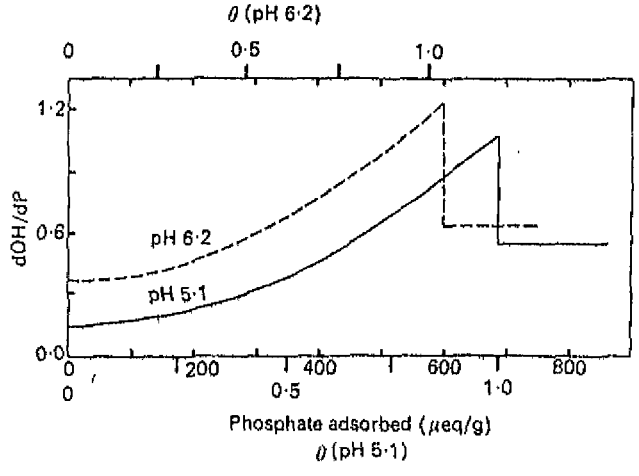

dOH/dP as a function of phosphate adsorbed and surface coverage, θ ($\theta = x/x_m$).

Figure 1.4.B

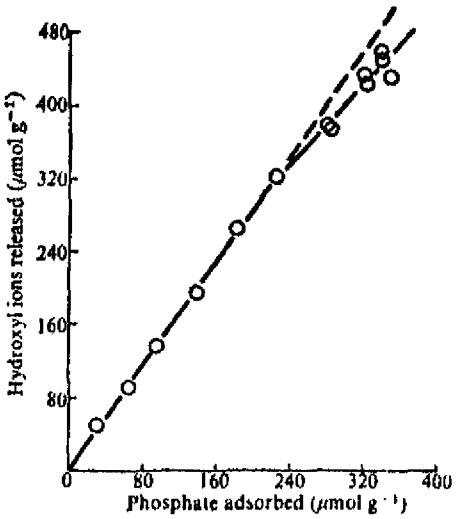

Hydroxyl ions released plotted against phosphate adsorbed. The two straight lines are drawn down according to the equations:
$OH^- = 1.44(\pm 0.05)P$ at $P < 212(\pm 40)$ μmol
$OH^- = 1.07(\pm 0.11)P + 79.3(\pm 33.4)$ at $P > 212$ μmol
Confidence interval 95%.

Figure 1.4.C

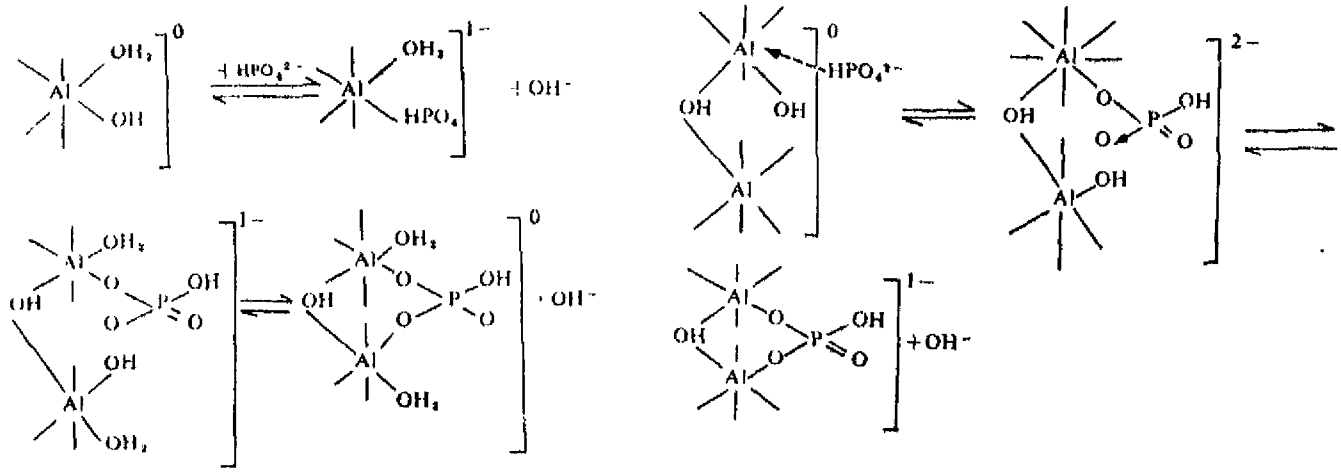

Scheme 1.2 from Rayan (1975)

The formation of bidentate bonds and the value of R.

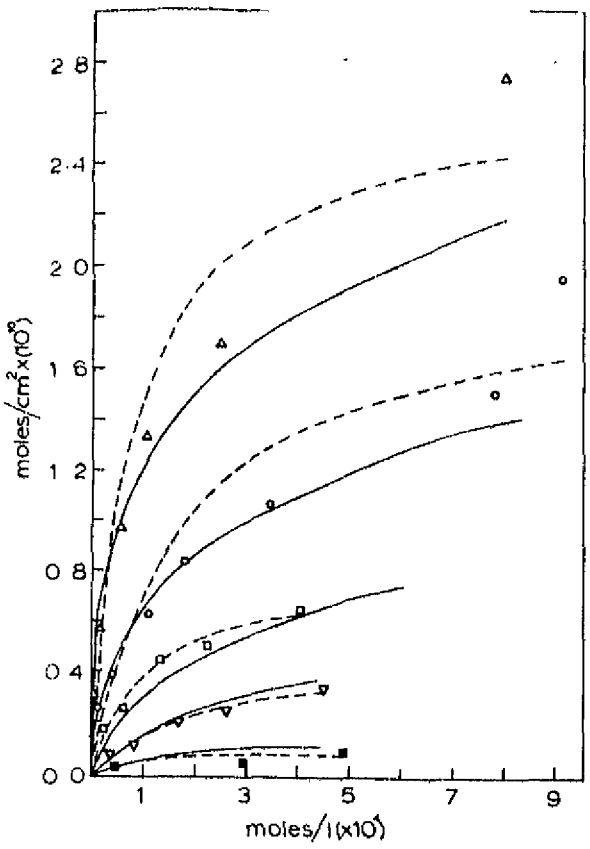

Adsorption isotherms of Zn(II) on goethite in 0.1 M NaCl. - - -, Langmuir isotherm; ——, present model. Points are from experimental data: ○, pH = 7.0; ◇, pH = 6.5; □, pH = 6.0; ▽, pH = 5.5; ■, pH = 5.0.

Figure 1.6.A

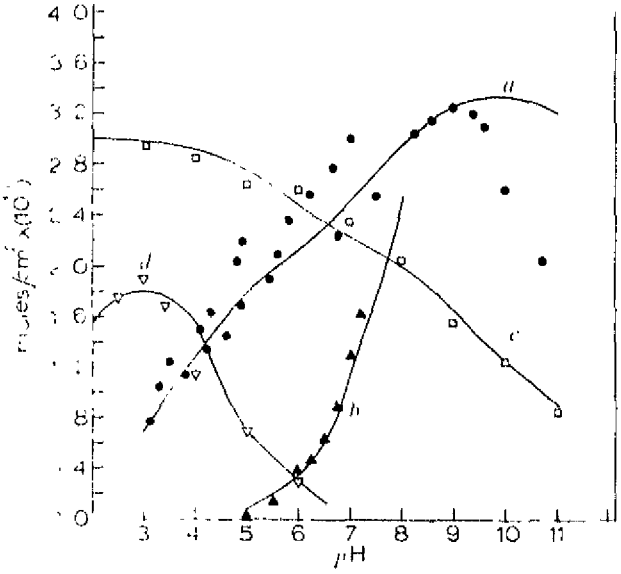

Adsorption on goethite as a function of pH. *a*, Silicate, 5 × 10⁻⁴ M (0.1 M NaCl); *b*, zinc, 1 × 10⁻⁴ M (0.1 M NaCl); *c*, phosphate, 3.2 × 10⁻⁴ M (0.01 M NaCl); *d*, 2,4-D, 3 × 10⁻⁴ M (0.01 M NaCl) — —, Present model. Points are from experimental data: ●, silicate; ▲, zinc; ▽, phosphate; ▼, 2,4-D.

Figure 1.6.B

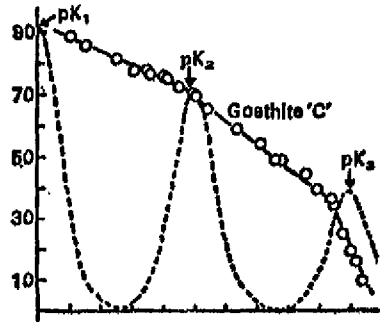

Figure 1.7 Adsorption envelope for phosphate on goethite at 20-23°C, using 0.1 g oxide per 25 ml 0.1 M NaCl. The dashed line is calculated by $X = 4\ V_m\ \alpha(1-\alpha)$

in which X = amount phosphate sorbed

V_m = max. adsorption capacity (for $\alpha = 0.5$ is $X = V_m$)

α = degree of dissociation of the acid

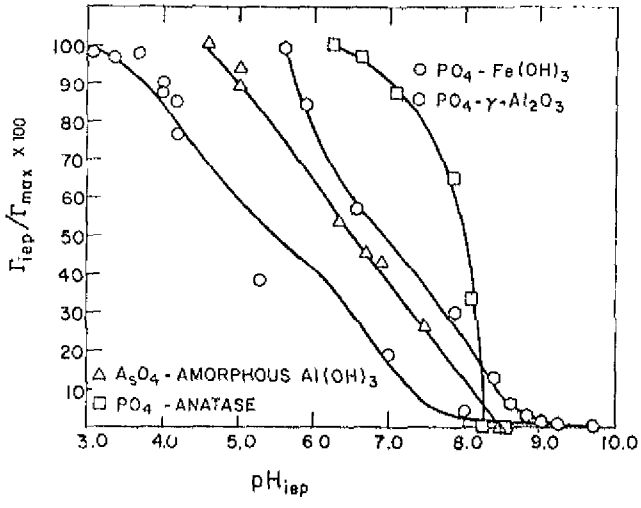

Fractional adsorption as a function of isoelectric pH. Experimental results and theoretical curves are depicted for each adsorption system. Adsorbent concentrations ranged from 0.13 to 0.16 g/liter. Initial adsorbate concentrations ranged from 0 to 1600 μM/liter; $NaClO_4$ concentration was 0.01 M/liter.

Figure 1.8 pH_{iep} = pH at the isolectric point

Γ_{iep} = the adsorption at pH_{iep}

Γ_{max} = the maximum adsorption

Reaction constants and adsorption maxima of the phosphate adsorption by 12 Dutch soils

Soil	$(\mu g/ml)^{-1}$		μg P/g soil			μg P/m^2 surface		
	b_1	b_2	P_{m1}	P_{m2}	P_m	P_{m1}	P_{m2}	P_m
1. Sticky soil	2.8	0.033	70	825	895	1.6	18.5	20.1
2. Loess soil	1.9	0.013	60	195	255	2.1	6.9	9.0
3. Wilh.p.soil	0.093	0.013	140	400	540	1.1	3.2	4.3
4. Oss soil					1600			22.0
5. River b.c.soil	1.1	0.029	60	850	910	0.3	4.7	5.0
6. Griend soil	1.2	0.005	100	535	635	1.3	7.3	8.6
7. Munnekeland soil	2.8	0.046	25	405	430	0.4	7.3	7.7
8. Randwijk soil					580			6.2
9. Wolfswaard soil	0.09	0.007	185	415	600	2.0	4.6	6.6
10.Y-polder soil	0.31	0.006	150	390	540	1.1	2.9	4.0
11.N.O.P. soil	0.56	0.008	50	230	280	0.7	2.9	3.6
12.Winsum soil	0.48	0.012	40	700	740	0.5	8.8	9.3

Table 2.1.1 Adsorption described by a double Langmuir equation

$$P_{ads} = \frac{b_1 C P_{m1}}{1 + b_1 C} + \frac{b_2 C P_{m2}}{1 + b_2 C}$$

Phosphate sorption properties of the soils, their clay fractions, and bottom sediments

Adsorbent	Adsorption (Pm) maximum	Adsorption (b) energy	EPC	P desorbed
	$\mu g/g$	$ml/\mu g$	$\mu g/ml$	$\mu g/g$
Soils:				
Roselms I	287	1.69	0.032	1.77
Broughton	209	4.89	0.008	0.46
Roselms II	249	2.85	0.017	0.57
Paulding	216	4.35	0.140	0.29
Lenawee	244	0.80	0.060	3.58
Blount	199	2.15	0.011	0.75
Hoytville	258	1.49	0.240	0.91
Soil clay fractions:				
Roselms I	393	0.86	0.034	2.21
Broughton	323	4.15	0.016	0.95
Roselms II	411	1.91	0.016	0.99
Paulding	455	1.09	0.008	1.12
Lenawee	422	0.82	0.032	3.68
Blount	538	7.43	0.006	1.13
Hoytville	623	1.63	0.008	1.18
Bottom sediments:				
Independence 1 Dec. 1975	222	1.00	0.035	3.98
Auglaize 11 Dec. 1975	4,870	0.68	0.054	3.61
Tiffin 1 Dec. 1975	1,930	1.55	0.026	1.33
Independence 24 Mar. 1976	3,580	1.05	0.024	1.42
Auglaize 24 Mar. 1975	4,550	1.36	0.024	1.81

Table 2.1.2 EPC = equilibrium phosphate concentration (amount phosphate adsorbed = amount phosphate desorbed P_{des} = phosphate desorbed after ten successive 6 hours desorption into 0.01 M CaCl at 10:1 suspension soil ratio.

Correlation coefficients among phosphate parameters and calcite content from the stream composited sediment samples (n = 13)

	Total P	Adsorption maximum	Adsorption energy	Total desorbed	EPC
Calcite content	0.674*	N.S.†	-0.559*	0.759**	0.888**
Total P		N.S.	-0.698**	0.872**	0.867**
Adsorption maximum			-0.663**	N.S.	N.S.
Adsorption energy				-0.794**	-0.714**
Total desorbed					0.950**

*,** Significant at the 5% and 1% level, respectively.
† N.S. = not significant.

Table 2.1.3

Sorption constants for regions (I, II, and III) of the overall P sorption isotherms obtained for Okaihau soil, Fe gel, and synthetic and natural goethite

, *obtained by resolution of isotherms using the Langmuir equation (ΔG is the free energy of sorption and b is the sorption maximum).*

	Sorption constants					
	ΔG_I	ΔG_{II}	ΔG_{III}	b_I	b_{II}	b_{III}
Time *h*	*kJ mol*$^{-1}$			*μ mol g*$^{-1}$		
			Okaihau soil			
40	-39.5	-29.7	-20.1	9.7	29.4	48.4
Equilibrium	-39.1	-30.2	-21.0	21.5	33.2	55.8
			Fe gel			
17	n.d.*	-29.1	-18.4	445	445	1020
305	n.d.	-29.1	-18.4	560	445	1020
			Synthetic goethite			
Equilibrium	-41.4	-32.1	-21.3	63.7	31.9	30.0
			Natural goethite			
48	n.d.	-31.3	-19.4	17.4	39.4	49.0
192	n.d.	-31.4	-19.5	32.3	40.6	51.6

*ΔG_I values for Fe gel and natural goethite could not be determined accurately, but the values for both sorption periods are approximately -45 kJ mol^{-1}.

Table 2.1.4

Sorption constants describing the three (I, II and III) regions of P sorption by four soils and Fe gel using different experimental conditions:
ΔG is the free energy of sorption (derived from the Langmuir sorption energy constant) and b is the sorption maximum

Sorbent	ΔG_I	ΔG_{II} kJ mole^{-1}	ΔG_{III}	b_I	b_{II} μmole g^{-1}	b_{III}
			Equilibrium; 10^{-1} M NaCl			
Egmont soil	-38.5	-29.9	-21.8	39.3	48.4	104
Okaihau soil	-39.1	-30.2	-21.0	21.5	33.2	55.8
Porirua soil	-37.0	-29.4	-19.3	4.2	9.2	17.1
Waikakahi soil	-36.8	-29.6	-22.5	1.4	2.6	10.5
Fe gel*	n.d.	-29.1	-18.4	590	445	1020
			40 h; 10^{-1} M NaCl			
Egmont soil	-36.5	-29.1	-21.2	20.3	26.8	94.8
Okaihau soil	39.5	29.7	20.1	9.7	29.4	48.4
Porirua soil	-39.3	-28.3	-19.9	1.6	7.4	15.5
Waikakahi soil	-38.3	-28.7	-20.3	0.6	2.5	9.1
Fe gel	n.d.	-29.7	18.4	480	450	1018
			40 h; 10^{-4} M NaCl			
Egmont soil	-41.3	-31.0	-21.2	8.0	18.1	37.4
Okaihau soil	-43.6	-29.6	-20.1	4.2	14.7	22.4
Porirua soil	-40.8	-31.1	-21.9	0.7	2.8	7.2
Waikakahi soil	-38.6	-29.8	-20.8	0.6	2.3	8.0
Fe gel	n.d.	-36.0	-19.0	226	242	643

* constants relate to sorption during 690 h; final pH = 7.0
\# not determined

Table 2.1.5

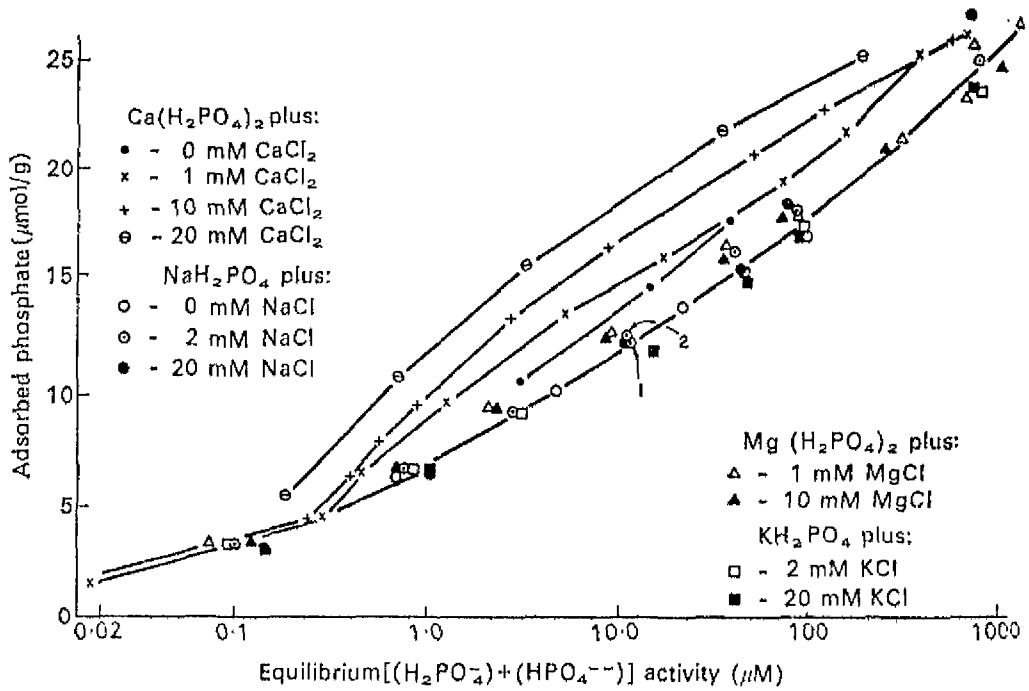

Effects of the Cl salts of Ca, Mg, Na, and K on P adsorption by gibbsite (24 h reaction at pH 5·5); 1 and 2, see text.

Figure 2.2.1

activity of HCO_3^- 0.30 10^{-3} and 0.44 10^{-3} respectively. Most of the points are falling in this range

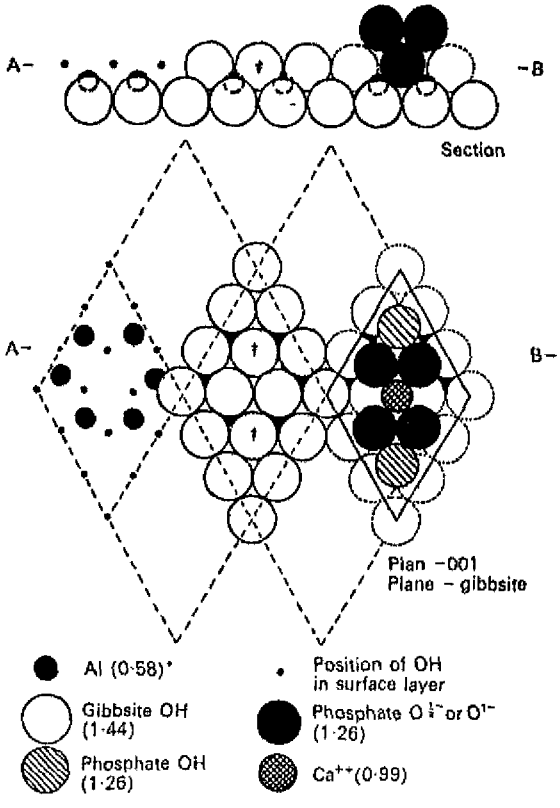

FIG. 3. Surface complex of adsorbed P and Ca.

‡ OH ions replaced by P molecules on the right hand side of the diagram.
* Number in parentheses is the ion radius in Å.
—— Outlines of surface 'unit cell' of the adsorbed complex area = 64·6 Å².
– – – Outlines adjacent areas where surface complexes could form.

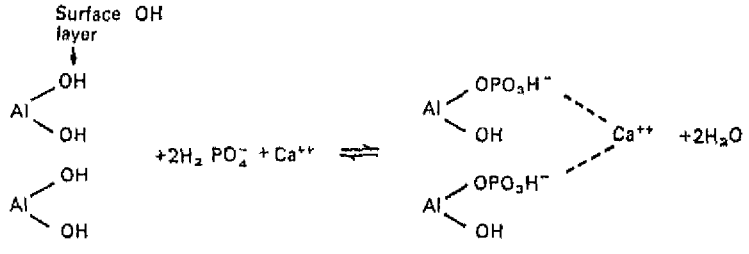

Proposed reaction of the adsorption of P and Ca by gibbsite.

Figure 2.2.2

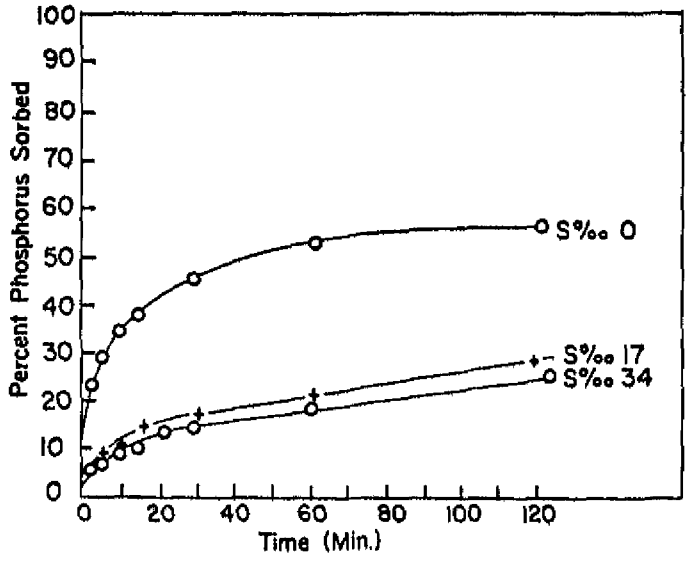

The effect of variations in salinity on the uptake of phosphorus. Initial conditions ; pH 3·4, solids 310, phosphorus 0·9 μ g-at P/l, salinity as noted.

Figure 2.2.3

Acid extractable Iron, Aluminium, Manganese, and Calcium

Clay	Fe mg/g	Al mg/g	Mn mg/g	Ca mg/g
Kaolinite 3	0.028	0.14	0.001	0.225
Montmorillonite 21	0.171	0.68	0.011	5.75
Illite 36	2.38	2.45	0.114	1.16

Composition of Systems in Adsorption Capacity studies

Clay	Init. phosphate mg/P/l	Solids concn. g/l	pH
Kaolinite 3	3.4-40	10-100	7-8
Montmorillonite 21	3.5-25	10	7.6
Illite 36	10-30	5	7.5

Adsorption capacities for the clay

Case	Adsorption capacity mg/g		95% confidence boundaries, mg/g
	Kaolinite 3		
No salt	0.091	0.082	ads.cap. < 0.102
0.03 M Na_2SO_4	0.19	0.111	ads.cap. < 0.259
0.498 M NaCl	0.148	0.132	ads.cap. < 0.168
	Montmorollinite 21		
No salt	0.746	0.693	ads.cap. < 0.807
0.03 M Na_2SO_4	0.751	0.624	ads.cap. < 0.943
0.498 M NaCl	0.697	0.639	ads.cap. < 0.766
0.03 M Na_2SO_4 and 0.498 M NaCl	0.873	0.800	ads.cap. < 0.962
	Illite 36		
No salt	2.51	2.20 <	ads.cap. < 2.92
0.03 M Na_2SO_4	2.35	2.24 <	ads.cap. < 2.47
0.498 M NaCl	2.56	2.29 <	ads.cap. < 2.90
0.03 M Na_2SO_4 and 0.498 M NaCl			

Table 2.2.1 Chemical properties, adsorption conditions and adsorption capacities for Kaolinite, Montmorillonite and illite (see fig. 2.2.4)

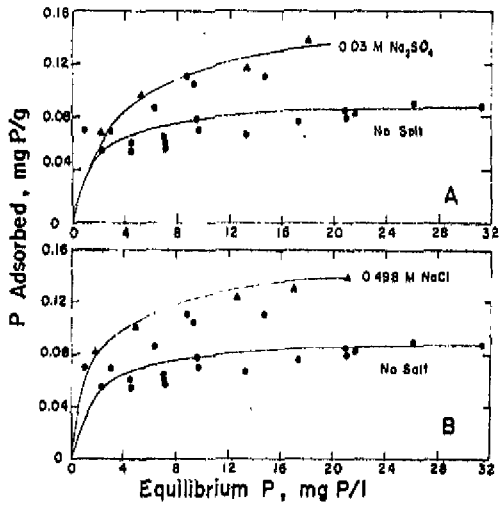

Effects of 0.03 M Na_2SO_4 (A) and 0.498 M NaCl (B) on phosphate adsorption on kaolinite at 28 ± 1 °C

Figure 2.2.4.A

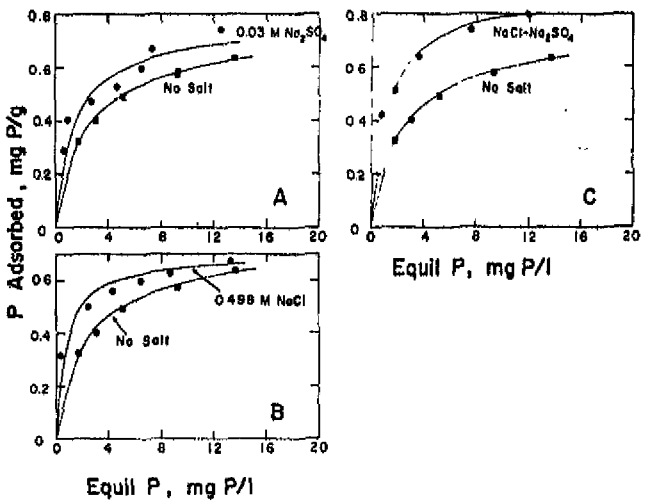

Effects of 0.03 M Na_2SO_4 (A), 0.498 M NaCl (B), and 0.498 M NaCl–0.03 M Na_2SO_4 (C) on phosphate adsorption on montmorillonite

Temperature was 25 °C for no salt case and 28 ± 2 °C for others

Figure 2.2.4.B

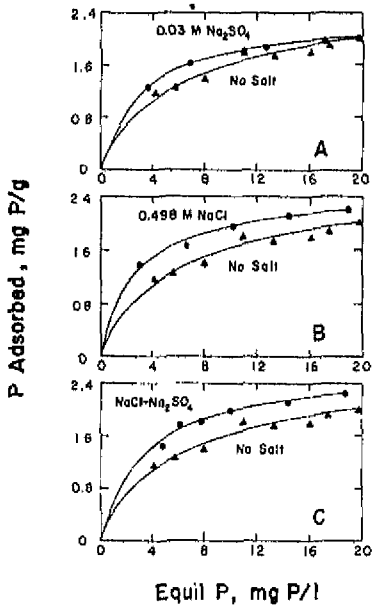

Effects of 0.03 M Na_2SO_4 (A), 0.498 M NaCl (B), and 0.49 M NaCl–0.03 M Na_2SO_4 (C) on phosphate adsorption on illite at 2 ± 1 °C

Figure 2.2.4.C

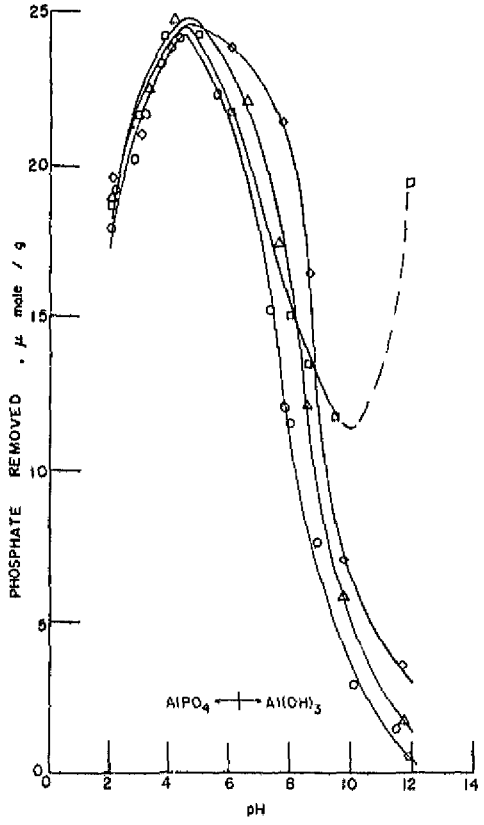

Effect of cations. α-Alumina, 0.6 g/130 ml, 25°. Initial phosphate concentration 1.15×10^{-4} *M* or 25 μmole g. Pre equilibration with 0.01 *M* NaCl, 1 hr; reaction with phosphate, 24 hr. ○ Phosphate only; □ 1.87×10^{-4} *M* $CaCl_2$ added; △ 1.54×10^{-5} *M* $La(NO_3)_3$ added; ◑ 46 mg/l Purifloc C-31 added.

A

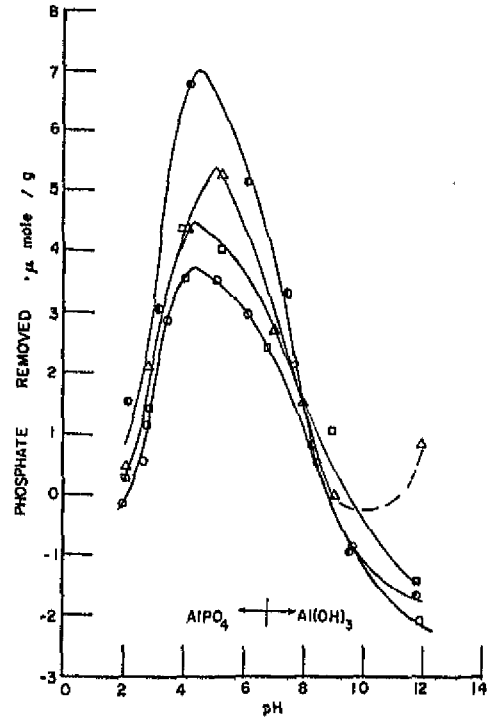

Effect of Cations. Kaolinite, 0.9 g/115 ml, 25°. Initial phosphate concentration 8.7×10^{-5} *M* or 11 μmole/g. Pre-equilibration with 0.01 *M* NaCl, 1 hr; reaction with phosphate, 24 hr. ◐ 34 mg/l purifloc C-31 added; △ 1.33×10^{-4} *M* $CaCl_2$ added; □ 1.33×10^{-4} *M* $La(NO_3)_3$ added; ○ phosphate only.

B

Figure 2.2.5.A-B

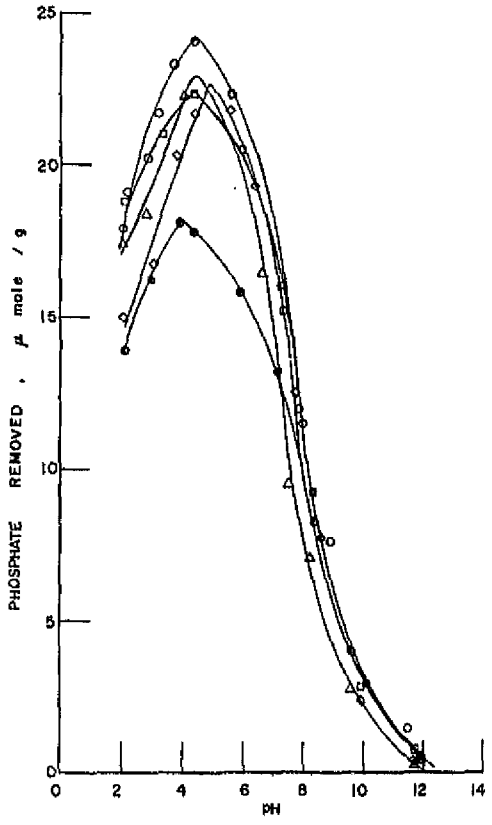

Effect of anions. α-alumina, 0.6 g/130 ml, 25°. Initial phosphate concentration 1.15×10^{-4} *M* or 25 μmole/g. Pre-equilibration with 0.01 *M* NaCl, 1 hr; reaction with phosphate, 24 hr. ○ phosphate only; △ 31 mg/l humic acid added; □ 3.75×10^{-4} *M* succinate added; ◇ 46 mg/l NaPSS added; ◐ 3.75×10^{-4} *M* NaF added.

C

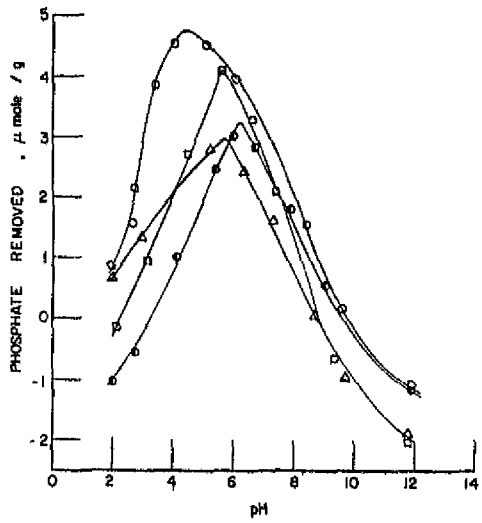

Effect of anions. Kaolinite, 0.9 g/115 ml, 25°. Initial phosphate concentration 8.75×10^{-5} *M* or 11 μmoles/g. Pre-equilibration with 0.01 *M* NaCl, 1 hr; reaction with phosphate, 24 hr. ○ phosphate only; □ 34 mg/l NaPSS; ◐ 1.33×10^{-4} *M* NaF; △ 34 mg/l Humic acid.

D

Figure 2.2.5.C-D

Sorption constants for the three (I, II, and III) regions of overall P sorption isotherms, obtained by resolution of P sorption data using the Langmuir equation, describing P sorption from different matrix solutions by Egmont and Porirua soils (ΔG is the free energy of sorption derived from the Langmuir sorption energy constant and b is the sorption maximum).

		ΔG_I	ΔG_{II}	ΔG_{III}	b_I	b_{II}	b_{III}
Soil	*Matrix solution*	kJ mole^{-1}			μmole g^{-1}		
Egmont	10^{-2} M Ca	−38.5	−29.4	−23.0	40.3	53.2	135
	1 M Na	−38.5	−29.8	−22.1	39.4	53.6	129
	10^{-1} M Na	−38.5	−29.3	−21.2	39.4	48.4	105
	3×10^{-2} M Na	−38.5	−29.3	−20.1	39.4	48.4	97.7
	10^{-2} M Na	−38.6	−29.4	−18.3	38.7	49.4	71.0
Porirua	10^{-2} M Ca	−37.1	−29.4	−20.1	4.19	9.19	20.6
	1 M Na	−37.1	−29.4	−20.5	4.19	9.19	18.7
	10^{-1} M Na	−37.1	−29.3	−19.3	4.19	9.19	17.1
	3×10^{-2} M Na	−37.1	−29.4	−18.6	4.19	9.19	14.0
	10^{-2} M Na	−37.1	−29.3	−18.6	4.19	8.94	7.68

Table 2.2.2

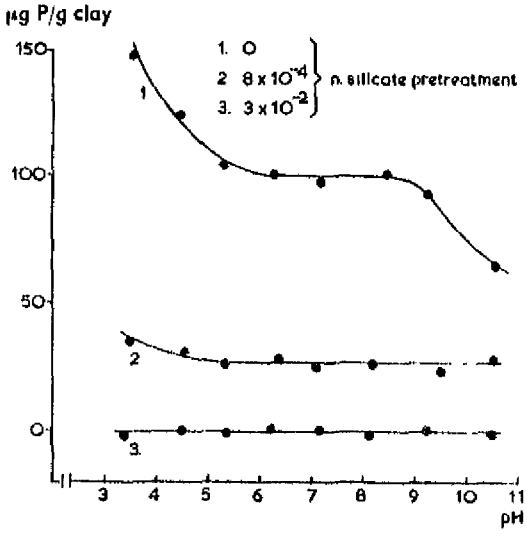

The adsorption of phosphate on Na-montmorillonite as a function of pH and silicate pretreatment

Figure 2.3.1

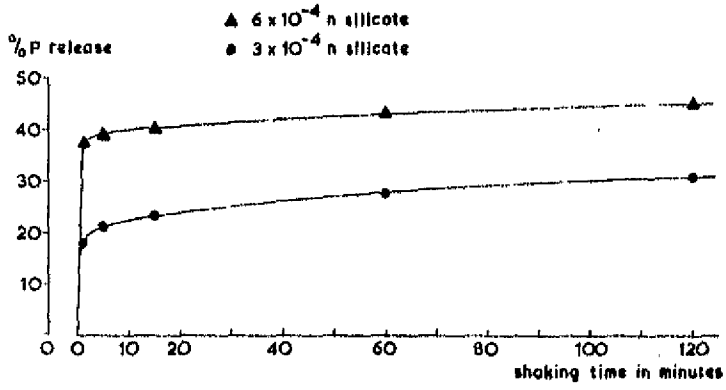

The release of pre-adsorbed phosphate against silicate as a function of time

Figure 2.3.2

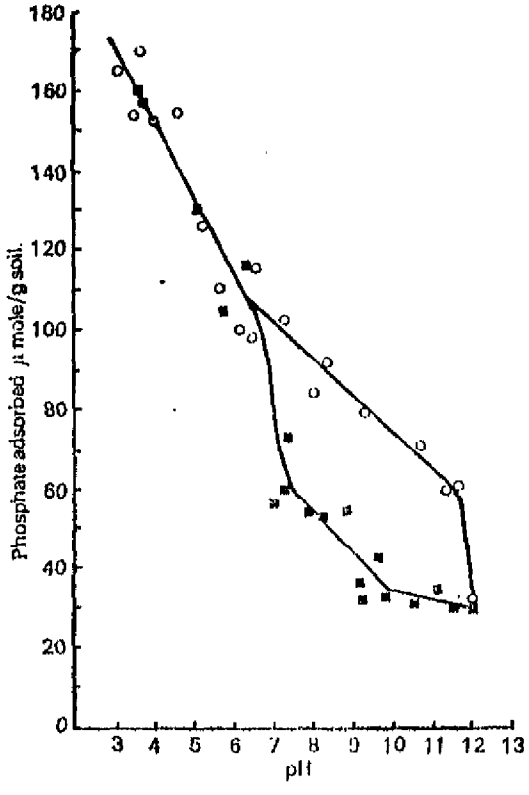

The effect of silicate on phosphate adsorption from mixed solutions Woodburn.

○ Silicate absent ■ Silicate present.

Figure 2.3.3

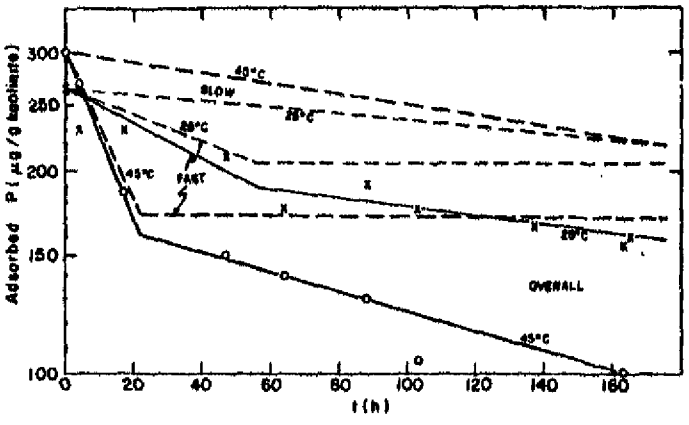

—Adsorbed P *(Ap)* as a function of desorption time *(t)* and temperature *(T)* (Expt. 2). Note the ordinate logarithmic scale. Overall reactions (solid lines) separated to fast and slow reactions (dotted lines) the first terminating after t_c hours. Solid curves calculated according to $Ap_T(t) = Ap_T(O)\,[\exp(-K_{S_T} \cdot t) + \exp(-K_{F_T} \cdot t) - 1]$ for $t \leq t_{c_T}$ and $Ap_T(O)\,[\exp(-K_{S_T} \cdot t) - a \cdot t_{c_T}]$ for $t > t_{c_T}$. $Ap_{25}(O) = 265$, $Ap_{45}(O) = 300$, $t_{c_{25}} = 50$ hours, $t_{c_{45}} = 22$ hours, $a(t_{c_{25}}) = 0.207$, $a(t_{c_{45}}) = 0.429$, K_{S_T}, K_{F_T};

Figure 2.3.4

at 25°C

$K_{S_{25°}} = 1.15\ 10^{-3}\ h^{-1}$

$K_{F_{25°}} = 4.65\ 10^{-3}\ h^{-1}$

at 45°C

$K_{S_{45°}} = 1.38\ 10^{-3}\ h^{-1}$

$K_{F_{45°}} = 25.5\ 10^{-3}\ h^{-1}$

Phosphate Removal Kinetics

Observed specific rate constants in the following slow reaction step

Kaolinite (surface area, 10.7 m^2/g)				*γ-Al_2O_3 (surface area, 10 m^2/g)*			
		K_{obs} (day $^{-1}$) at 50°C					
Solids concn, g/l.	pH	First phosphate addition	Second phosphate addition	Solids concn, g/l	pH	K_{obs} (day $^{-1}$) At 50°C	At 25°C
7.5	3.5	0.0560	0.0587	2.5	3.5	0.0329	0.0240
7.5	4.6	0.0224		2.5	4.3	0.0219	
15.0	4.6	0.0398	0.0550	2.5[a]	4.3	0.0219	
7.5	5.3	0.0110		2.5	6.0	0.0071	
7.5	6.2	0.0030		2.5	8.5	0	
7.5	7.5	0					

[a] 1.0×10^{-4} *M* fluoride added.

Table 2.4.1

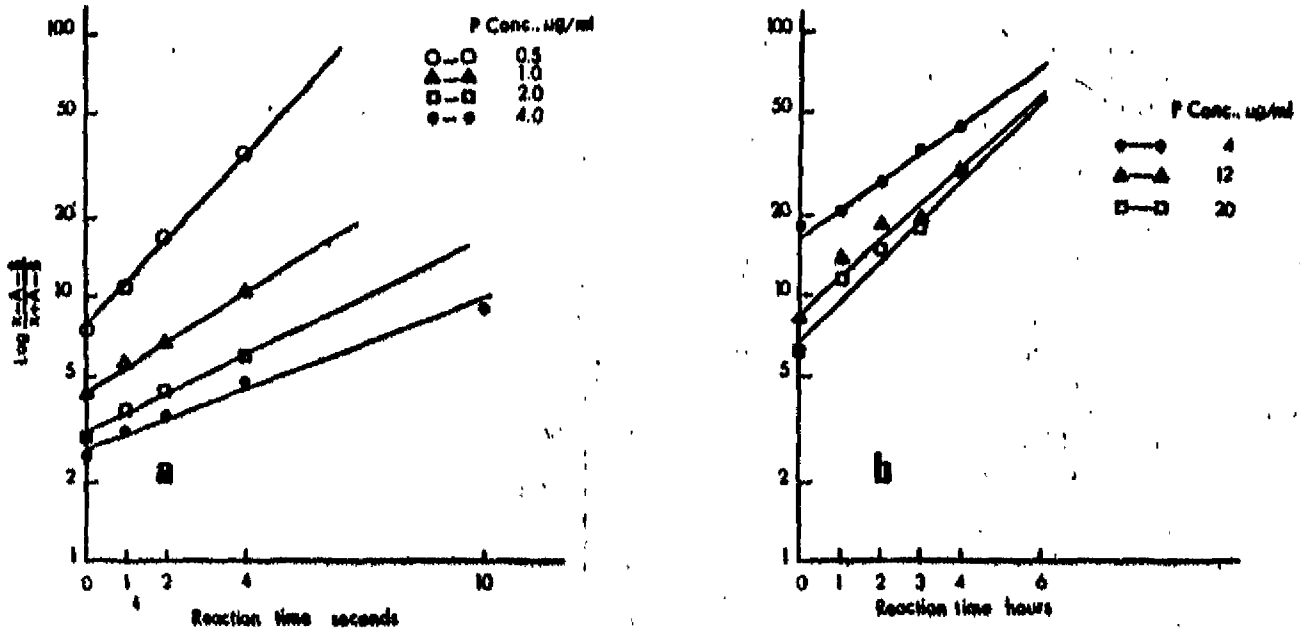

—Plot of the kinetic data of phosphate adsorption by (*a*) $CaCO_3$, and (*b*) Ca-kaolinite according to equation

Figure 2.4.1

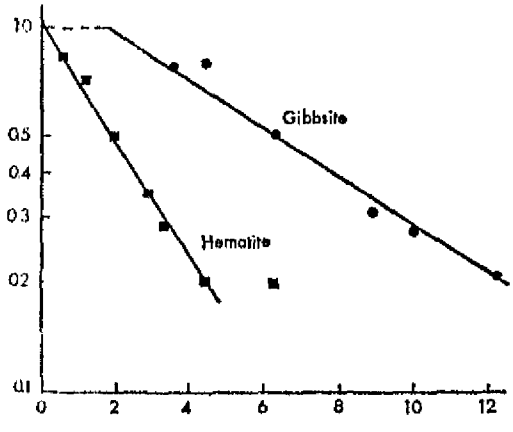

Plot of K on a logarithmic scale vs. $\sqrt{c}$

Figure 2.4.2

Initial P concentration	k_1	
	$CaCO_3$	Ca-kaolinite
ppm	1/ppm second	1/ppm hour
0.5	0.12	
1	0.086	
2	0.070	
4	0.043	0.0058
12		0.0095
20		0.0117

pH = 5 25°C

Rate constants of phosphate adsorption by $CaCO_3$ and Ca-kaolinite

Table 2.4.2

Sediment no.	pH (paste)	Sands +50µm	Coarse silt 50-20µm	Medium and fine silt 20-2µm	Coarse clay 2-0 2µm	Medium and fine clay -0 2µm	Organic matter	Oxalate-extr. Fe	DCB-extr. Fe	Total Fe	Total P	Organic P
		%									ppm	
12	4.61	2.6	26.9	50.0	13.2	7.3	18.3	1.0	1.18	3.36	1.240	535
14	4.65	51.5	23.3	17.8	4.0	3.3	11.5	0.56	0.57	2.00	660	452

Table 2.4.3 Physical and chemical properties of the sediments

Values obtained when Eq. 4.12Awas fitted to the changes in concentration of phosphate when soils were incubated at 25°C

Soil no.	pH in 0.01 M CaC_{12}	Proportion of variation acc. for	No. of obs.	Phosphate adsorbed (αgP/gsoil)	Coefficients of Eq. 4.12A			Equivalent values primary coefficients	
					K_o	K_1	K_2	b_1	b_2
1	5.9	0.991	22	1565	-18.4	2.51	0.543	0.216	0.399
2	4.4	0.996	16	1334	-19.6	2.73	0.538	0.197	0.366
3	5.8	0.990	19	1294	-20.0	2.79	0.564	0.202	0.359
4	6.3	0.996	18	1290	-19.3	2.69	0.608	0.226	0.371
5	5.7	0.984	18	1150	-17.3	2.45	0.571	0.233	0.407
6	5.3	0.995	21	939	-17.8	2.61	0.681	0.229	0.376
7	5.6	0.991	18	920	-17.2	2.52	0.528	0.209	0.397
8	5.7	0.987	22	507	-16.8	2.70	0.617	0.228	0.370
9	5.1	0.988	20	467	-15.7	2.55	0.780	0.306	0.392
10	5.3	0.989	22	394	-15.4	2.58	0.714	0.277	0.387
11	6.0	0.998	21	368	-16.1	2.72	0.685	0.252	0.367
12	4.8	0.984	22	275	-14.4	2.57	0.579	0.225	0.389
13	5.4	0.993	28	227	-13.4	2.46	0.658	0.267	0.406
14	5.2	0.992	20	194	-12.8	2.43	0.491	0.202	0.412
15	4.5	0.996	20	182	-13.9	2.66	0.608	0.228	0.376
16	4.5	0.996	19	108	-13.7	2.93	0.542	0.185	0.340
17	4.6	0.990	20	78	-11.5	2.64	0.413	0.156	0.378

Fitted value for the phosphate required to give a concentration of 1 μg P/ml of solution after 1 day.

Table 2.4.4A
*) Equation 4.12.A: $\ln A_t = k_o + K_2 \ln P - K_3 \ln t$, see text, Temperature of incubation constant: $K_o = K_1 + K_4/T$.

Values obtained when Eq. 4.12was fitted to the changes in concentration of phosphate when soils were incubated at a range of temperatures

Soil no.	Proportion of variation acc.for	No. of obs.	Coefficients of Eq. 4.12				Equivalent values of primary coefficients		
			K_1	K_2	K_3	K_4	b_1	b_2	cal. E/mole
1	0.992	12	-36.4	-	0.676	5465	0.269	-	16070
4	0.985	12	-41.3	-	0.655	6610	0.243	-	20060
5	0.997	12	-37.1	-	0.687	5940	0.280	-	17160
6	0.987	48	-42.2	2.85	0.704	6673	0.247	0.351	18820
7	0.986	12	-34.3	-	0.647	5463	0.270	-	16780
9	0.982	12	-39.2	-	0.872	7105	0.342	-	16190
11	0.994	12	-39.6	-	0.742	7078	0.273	-	18940
13	0.990	84	-35.4	2.45	0.600	6551	0.245	0.408	18940
16	0.900	11	-32.4	-	0.604	5556	0.206	-	18290

For these soils the range of values for added P was limited and the value of B_1 and hence b_2 was fixed at the value recorded in Table 2.4.4.A.

Table 2.4.4.B

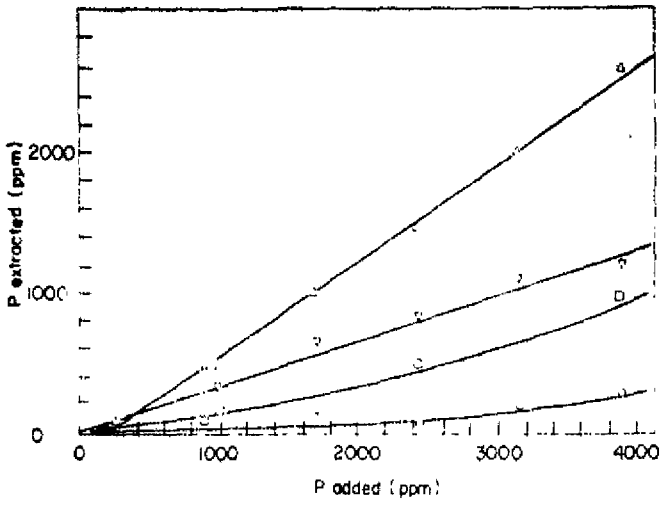

Figure 2.5.1 pH= 4, 20 °C

1 g soil extracted by 30 ml solution; Or 5 g resin in 100 ml

Phosphate extracted by different agents from Venezualan soil at various rates of added P. $^{\Delta}$, 0.02 citric acid; $^{\nabla}$, 0.0025 M citric acid; resin; .0.02 KCl

Influence of pH on release of phosphorus from lake sediments

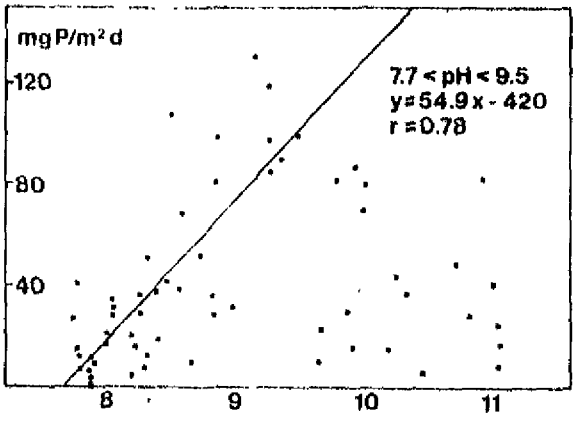

Rate of net orthophosphate release from undisturbed Kvind sø sediment at 20 °C.

Figure 2.5.2.A

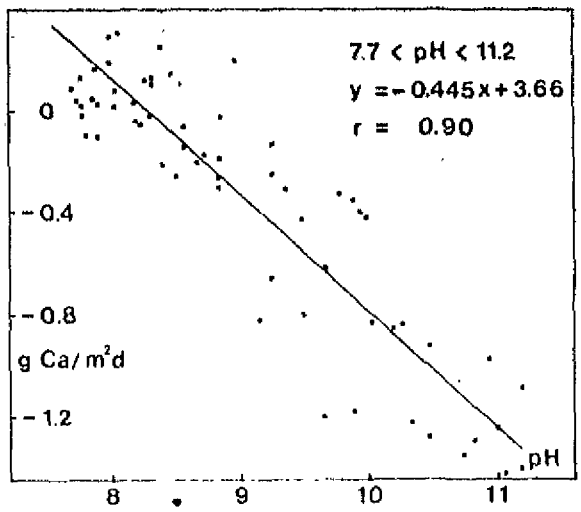

Rate of net calcium release from undisturbed Kvind so sediment at 20°C

Figure 2.5.2.B

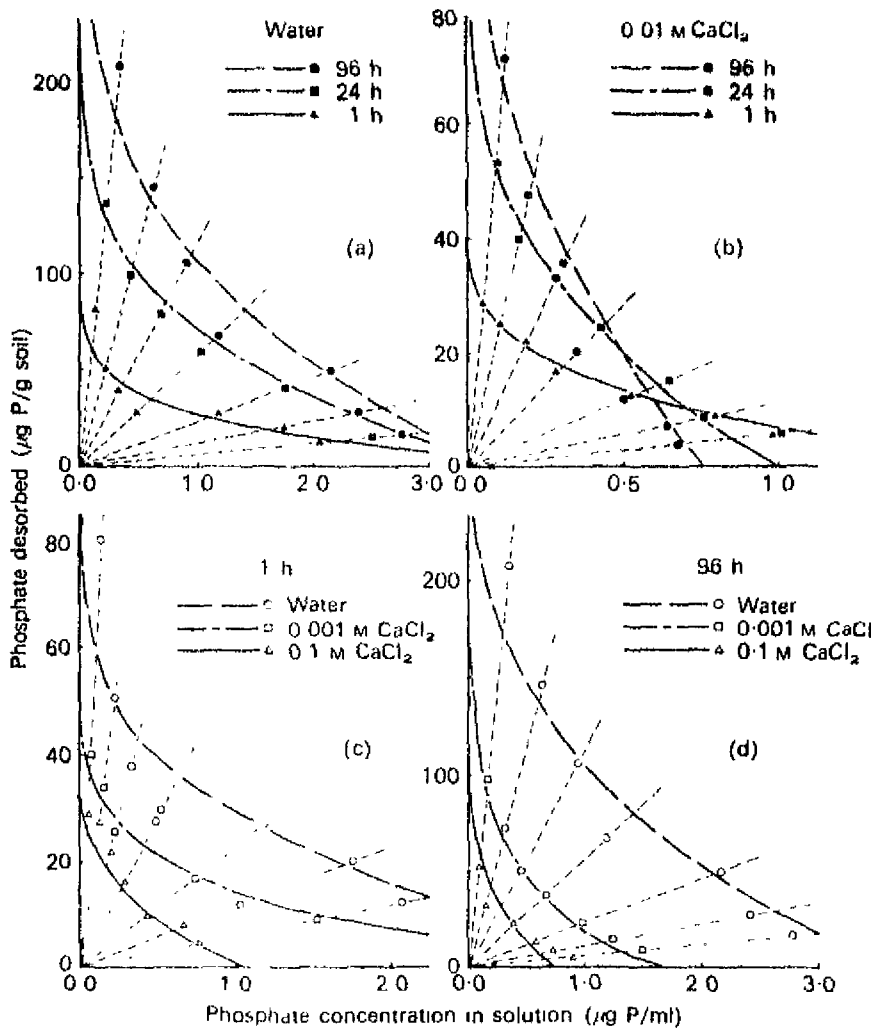

Figure 2.5.3.A

Relation between phosphate desorbed and solution concentration of phosphate. The conditions of measurement are summarized on each graph. The curves represent the individual equations summarized in Table 1. The radiating dashed lines represent given solution: soil ratios as described by equation 5.1. The values for these ratios, in anti-clockwise sequence, are: 6, 12, 24, 60, 120, 240, and 600. The intersection of the curves with the radiating lines indicate simultaneous solutions to Eq. (1) and (2) and thus the fitted values for adsorbed phosphate under given experimental conditions (see Table 2.5.1). Properties of the soil: yellowish brown loame sand, pH in 0.01 M $CaCl_2$ 5.6, pH in water (5:1) 6.2 total N 0.06% extractable Fe and Al 0.2 and 0.18%.

Summary of regressions fitted to describe desorption of phosphate at five calcium concentrations*

Initial calcium concentration (M)	*No. of observations*	K_p	m	a_1	n	b	R^2
0	35	97 7	0.300	67.9	0.308	0.257	0.976
0.001	35	55.2	0.279	40.1	0.315	0.277	0.984
0.005	35	52.1	0.268	44.4	0.312	0.327	0.973
0.01	35	42.8	0.280	35.6	0.338	0.320	0.987
0.1	32	40.0	0.290	39.0	0.325	0.363	0.972
Combined equation (1)	172	**	0.276	40.5	0.312	0.289	0.9785
(2)	172	†	0.263	40.0	†	0.315	0.9801

*The regressions fitted at each calcium concentration were the simultaneous equations:

$$1.\ P_d = K_p t_d^m + a_2 t_d^n c^b$$

$$2.\ P_d = cS$$

where P_d is the phosphorus desorbed ($\mu P/g$ soil); t_d is the period of desorption (h), c is the solution concentration of phosphate ($\mu P/cm^3$), and S is the solution:soil ratio (cm^3/g).
**For this equation, K_p was replaced by: $44.1 + (1/(0.0288 + 58.1\ Ca))$ and n by: $m + 0.0483(1 - 1/(1 + 1520\ Ca))$ where Ca is the final cation concentration (M).
†For this equation, K_p was replaced by: $44.9 + (1/(0.0335 + 63.3\ Ca))$.

Table 2.5.1

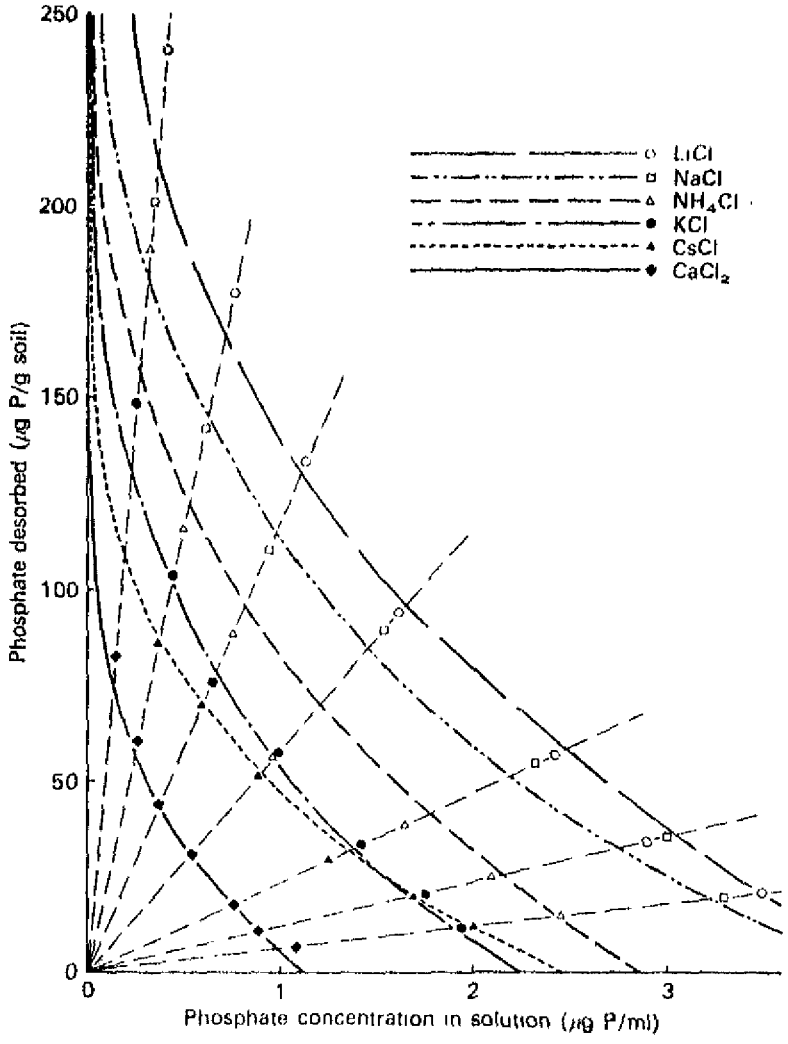

Desorption of phosphate after 96 h, and at the seven solution: soil ratios indicated in fig. 2.5.3.A by 0.03 M solutions of monovalent chlorides and by 0.01 M calcium chloride. The equations to the lines are summarized in Table 2.5.2. Values for rubidium chloride fall close to those for caesium chloride and have been omitted from the figure.

Figure 2.5.3.B

Summary of regressions * fitted to describe desorption of phosphate in 0.03 M solutions of monovalent cations and by 0.01 M calcium chloride

Salt present	No of observations	K_p	m	G_2	n	b	R^3
LiCl	21	110	0.314	74.0	0.323	0.246	0.993
NaCl	21	85.4	0.310	52.7	0.330	0.286	0.992
NH_4Cl	21	79.6	0.281	52.5	0.296	0.332	0.982
KCl	20	74.2	0.303	54.9	0.324	0.260	0.996
RbCl	18	75.2	0.304	58.4	0.314	0.335	0.990
CsCl	18	59.4	0.281	51.0	0.257	0.290	0.992
$CaCl_2$	21	59.7	0.209	52.5	0.229	0.315	0.996

* The regressions fitted were the simultaneous equations:

$$P_d = K_p t_d^m - a_2 t_d^n c^b$$
$$P_d = cS$$

where the symbols have the same meaning as in Table 2.5.1

Table 2.5.2

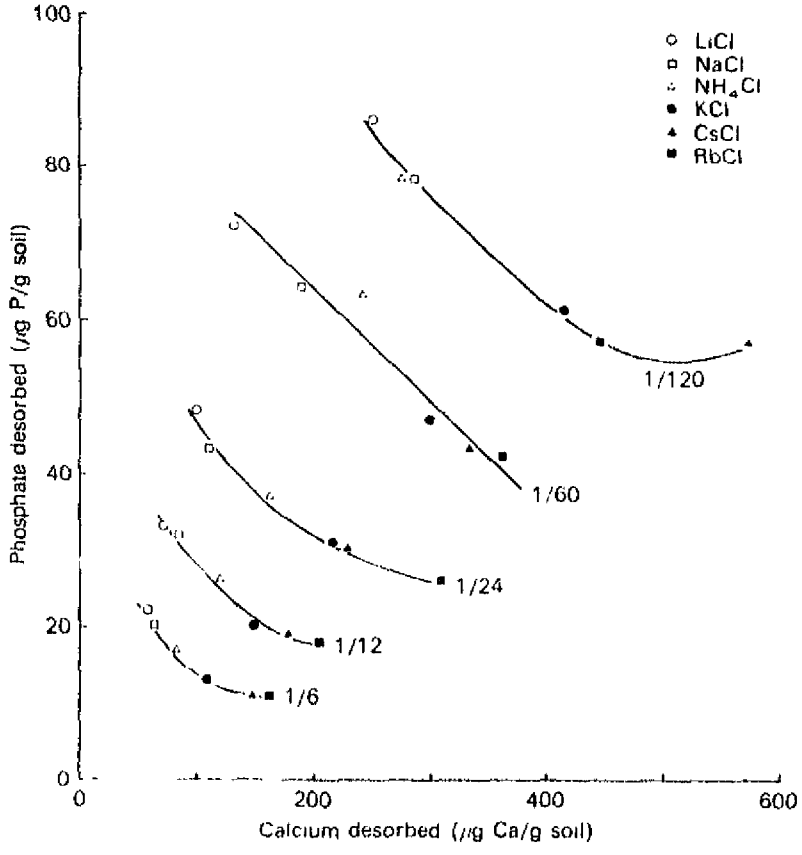

Relation between phosphate and calcium desorbed after 24 hours by 0.03 M solutions of monovalent salts at the indicated soil: solution ratios. The lines indicate regressions fitted through each set of points.

Figure 2.5.3.C

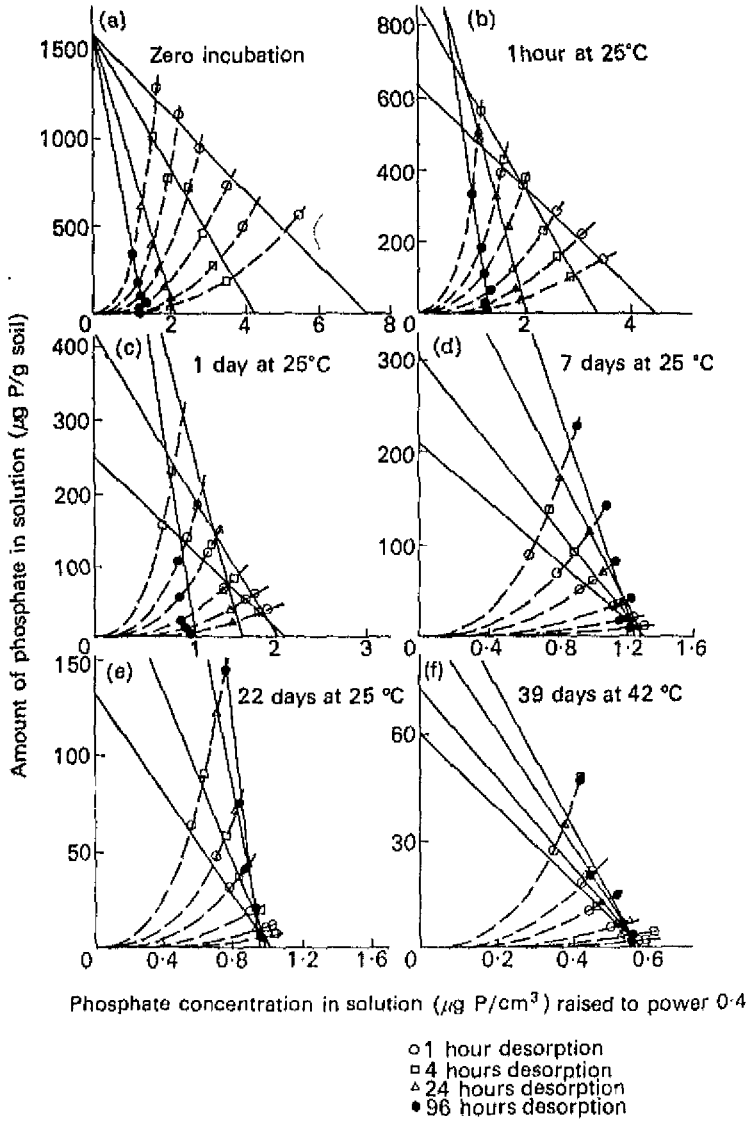

Figure 2.5.4

Effect of the indicated periods of incubation and of period of desorption on the amount of phosphate in solution - that is, on the phosphate desorbed. The equations to the lines summarized in Table 2.5.3. Values for 48 h and 72 h were used in fitting the equations but have been omitted from the diagrams to improve clarity.

Coefficients when equations 5.4, 5.5 and 5.3 were used to describe desorption of phosphate through 96 h after various periods of incubation

Period of incubation (days)	Temperature of incubation (°C)	Equivalent period at 25°C (days)	a_2	b_2	b_1 $c_{o,o}$	k	b_3	R^2
0.042	25	0.042	143	0.43	5.4	0.91	0.31	0.997
10	5	0.88	145	0.38	2.11	0.045	0.36	0.994
1	25	1.0	114	0.42	2.2	0.043	0.41	0.978
30	5	2.6	152	0.33	1.62	0.015	0.36	0.996
7	25	7.0	168	0.26	1.28	0.002	0.23	0.991
97	5	8.5	129	0.46	1.25	0.006	0.39	0.990
3	42	19.0	143	0.31	1.05	0.004	0.49	0.978
22	25	22.0	146	0.32	1.04	0.002	0.41	0.0997
10	42	62.0	146	0.23	0.79	0.0006	0.44	0.983
39	42	240.0	95	0.14	0.63	0.0002	0.39	0.988

Table 2.5.3

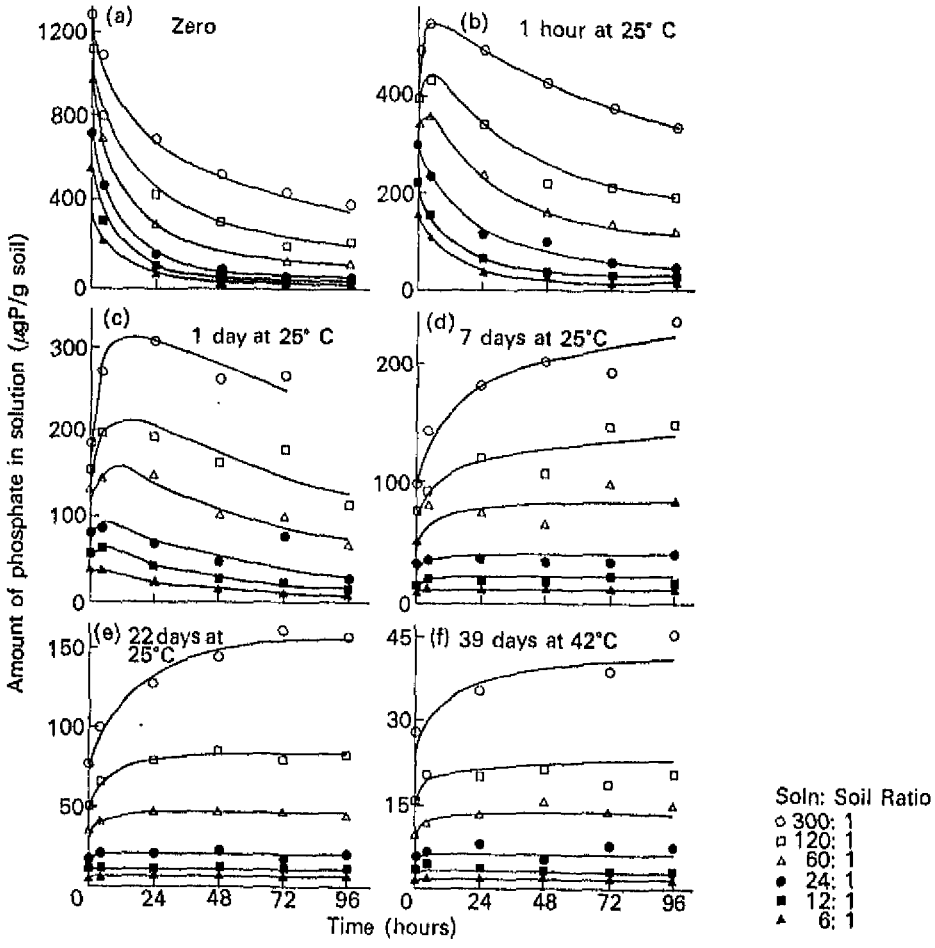

Changes through time in the amount of phosphate in solution after various periods of prior incubation. The equations to the lines are summarized in Table 2.5.3 and equations 5.3, 5.4, 5.5.

Figure 2.5.5

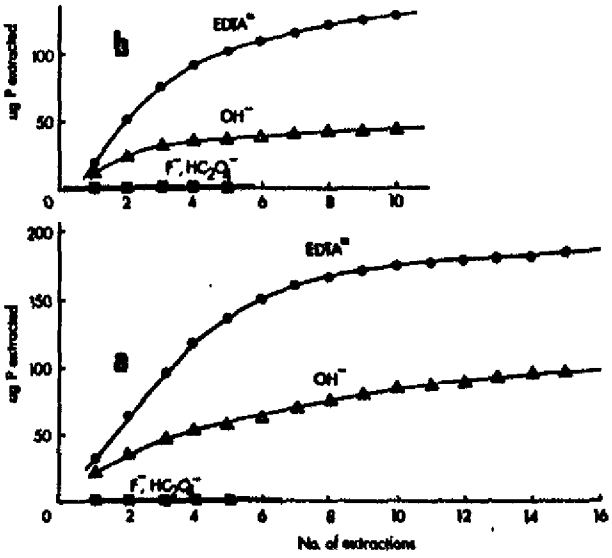

—The release of phosphorus from untreated sediments 12(*a*) and 14(*b*) by consecutive extractions with various dilute anionic solutions at 25C.

Figure 2.5.6.A For properties of sediments 12 and 14 see table 2.4.3

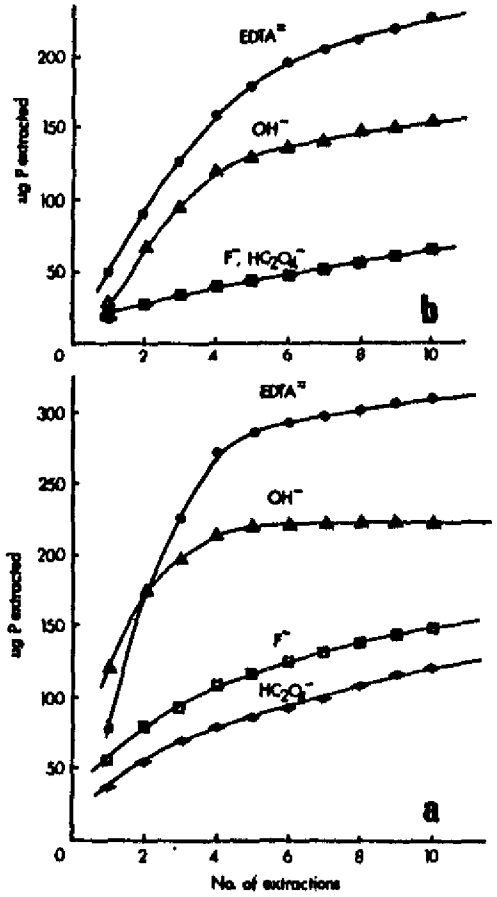

—The release of phosphorus from phosphated sediments 12(*a*) and 14(*b*) by consecutive extractions with various dilute anionic solutions at 25C.

Figure 2.5.6.B

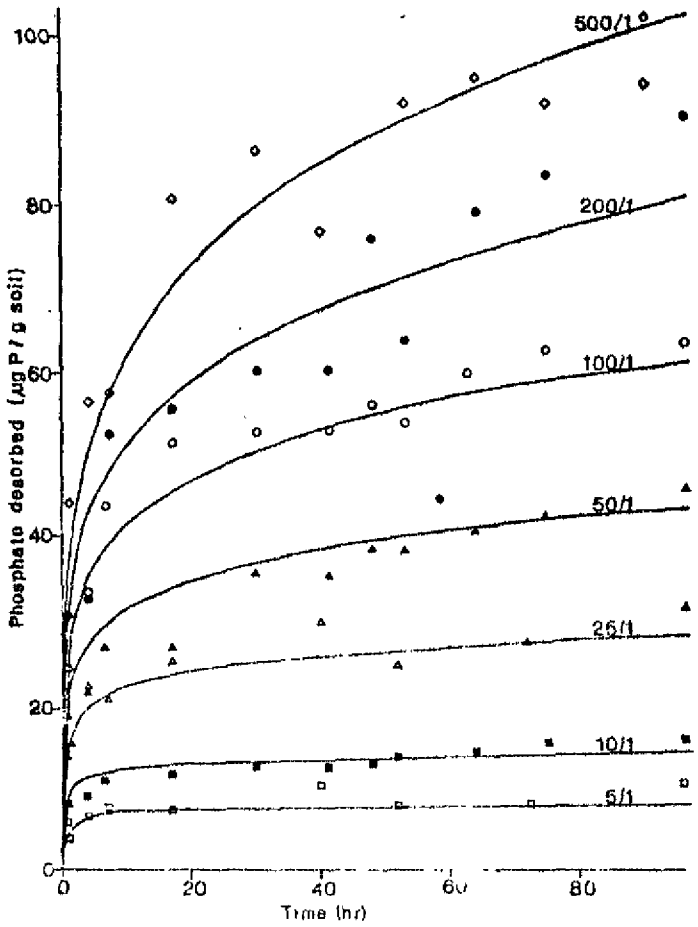

Comparison between the observed rate of desorption of phosphate from the Bakers Hill soil and that predicted from Eq. 1). The values of the parameters were those estimated using Eq.5.7. The calculating lines were obtained by finding values for desorbed phosphate (C_2) at a given period (t_d) which satisfied Eq. 1) subject to the provision that $P_d = A_t S$ where S is the solution: soil ratio and A_t is the concentration of phosphorus in solution. The soil had been incubated with phosphate at 1000 µgP/g soil for 18 days at 42°C.

Figure 2.5.7

eq.1) is a rewritten version of 5.7:

$$P_d = k_1(A_t^{b_1} - A_o^{b_1})\, t_d^{b_2}$$

Where A_o = concentration of phosphate in solution before desorption:

$$A_o = k_2 t_i^{-b_3} P_i$$

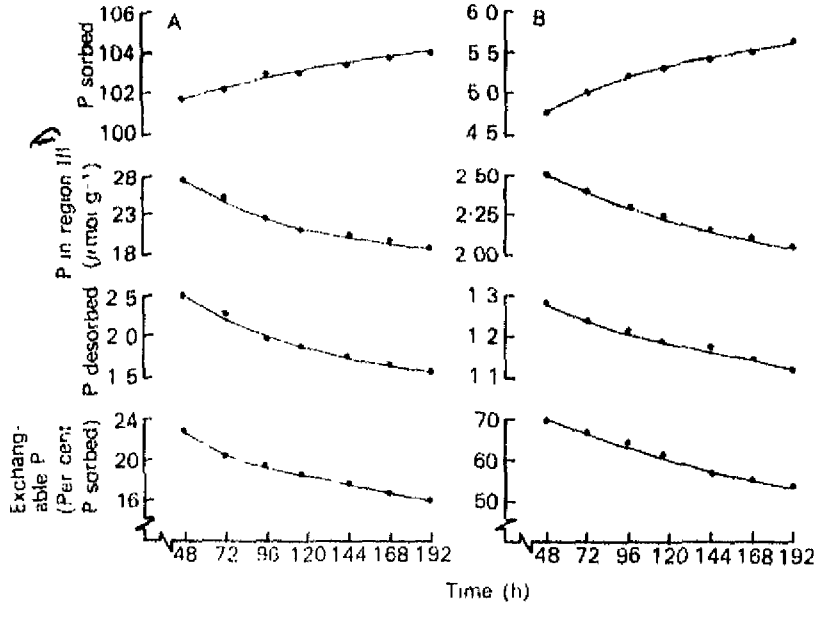

Changes in the overall amount of P sorbed, the amount of P sorbed in region III, the amount of P desorbed during 16 h, and the percentage of sorbed P which is isotopically exchangeable during 30 min, with increasing sorption time for (A) Egmont, and (B) Waikakahi soils.

Figure 2.5.8

1) P = region III = weakly bound phosphate see table 2.2.2, table 2.1.5 and table 2.1.4.

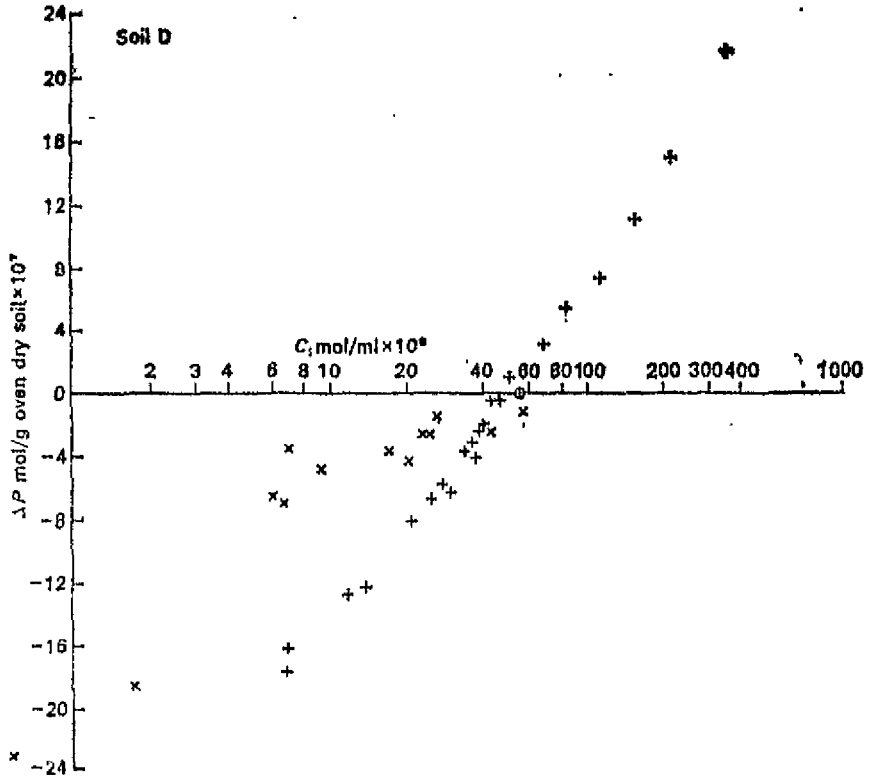

Soil D—Solution desorption (×); resin desorption (+); adsorption isotherms (+); for phosphate in 0·01M $Ca(NO_3)_2$.

Figure 2.5.9

Equations of the form, $\ln C_l = a + b\Delta P$ fitted to data.
C_l = P conc. in solution, mol per ml $\times 10^{-9}$
ΔP = quantity of P adsorbed by soil, mol per g oven dry soil $\times 10^{-7}$

Soil	*Isotherm method*	*Fitted constants*		*95% confidence interval for fitted value of b*
		a	*b*	±
B	Solution	2·55	0·226	0·027
	Resin	2·77	0·160	0·092
	Adsorption	2·71	0·106	0·015
C	Solution	3·55	0·168	0·012
	Resin	3·60	0·095	0·018
	Adsorption	3·50	0·093	0·010
D	Solution	3·80	0·206	0·044
	Resin	3·93	0·112	0·0081
	Adsorption	3·87	0·097	0·0150
E	Solution	7·26	0·035	0·0040
	Resin	7·21	0·028	0·0060

Table 2.5.4

COMPARISON OF PARAMETERS FOR LANGMUIR ISOTHERM

pH	γ – Al_2O_3 (117 $m^2 g^{-1}$)[a]			α – Al_2O_3 (10 $m^2 g^{-1}$)[c]			Gibbsite (48 $m^2 g^{-1}$)[d]			$Al(OH)_3$[e]
	Γ_m (μmole g^{-1})	K_L	$\bar{A}$ (Å^2)[b]	Γ_m (μmole g^{-1})	K_L	$\bar{A}$ (Å^2)	Γ_m (μmole g^{-1})	K_L	$\bar{A}$ (Å^2)	K_L
2	328	31,300	36	—	—	—	—	—	—	—
3	334	39,000	35	—	—	—	450	1.1	17	—
3.7	—	—	—	23	200	38	—	—	—	—
4	345	46,400	34	—	—	—	—	—	—	—
5	328	41,800	36	—	—	—	346	0.78	22	1.0
5.6	—	—	—	36	244	59	—	—	—	—
6	276	40,800	42	—	—	—	—	—	—	1.0
6.3	—	—	—	42	200	69	—	—	—	—
7	236	24,500	50	—	—	—	—	—	—	1.1
7.5	—	—	—	54	135	90	—	—	—	—
8	190	23,600	62	—	—	—	—	—	—	—
9	155	21,800	76	—	—	—	129	0.9	60	—
10	104	21,500	112	—	—	—	85	0.54	91	—
10.6	—	—	—	89	—	184	—	—	—	—
11	85	16,200	138	—	—	—	—	—	—	—

a. Huang (1975)
b. $\bar{A}$ = surface area occupied per adsorption site
c. Chen, Butler and Stumm (1973 B)
d. Muljadi, Posner and Quirk (1966)
e. Hsu and Rennie Canad. J. Soil Sci 42 (1962) 197

Table 2.6.1

Linear correlation coefficients and constants calculated from equation 6.2 for the oxides studied here

Oxide	r	C_1	μ^o_{total}
Gibbsite	0.9467***	4.99×10^{-3}	13,986
Boehmitte	0.8145*	2.94×10^{-4}	16,562
Corundum	0.9213***	1.31×10^{-3}	21,508
Goethite	0.9786***	8.38×10^{-3}	29.269
Lepidocrocite	0.9913***	1.66×10^{-2}	18,294
Hematite I	0.8604**	1.65×10^{-4}	30,652
Hematite II	0.9573***	2.80×10^{-3}	18,669
Anatase	0.9442***	5.07×10^{-3}	11,055
Pyrolusite	0.9736***	1.90×10^{-4}	20,234

Table 2.6.2

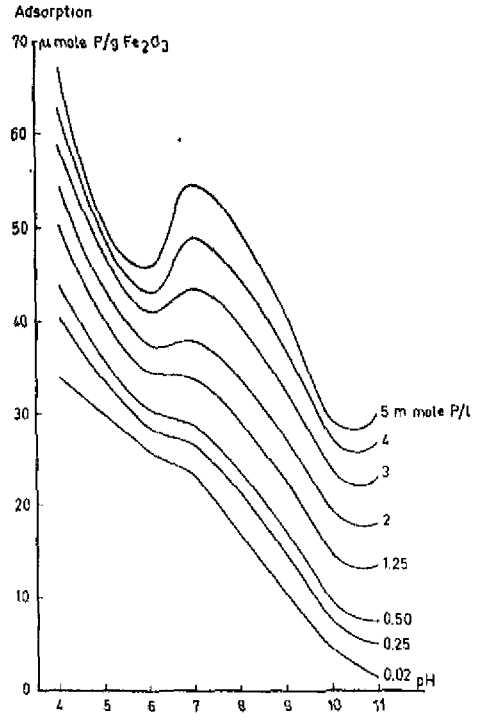

Adsorption of phosphate on hematite. Effect of pH at various concentrations of phosphate

Figure 2.6.1

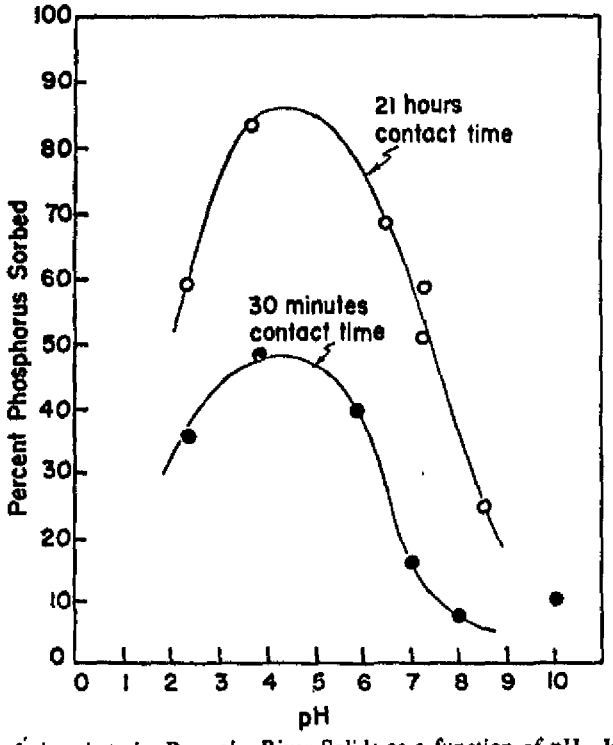

Removal of phosphate by Roanoke River Solids as a function of pH. Initial conditions ; temperature 21°C, solids 310 ppm, total phosphorus 0·5 μ g-at P/l.

Figure 2.6.2

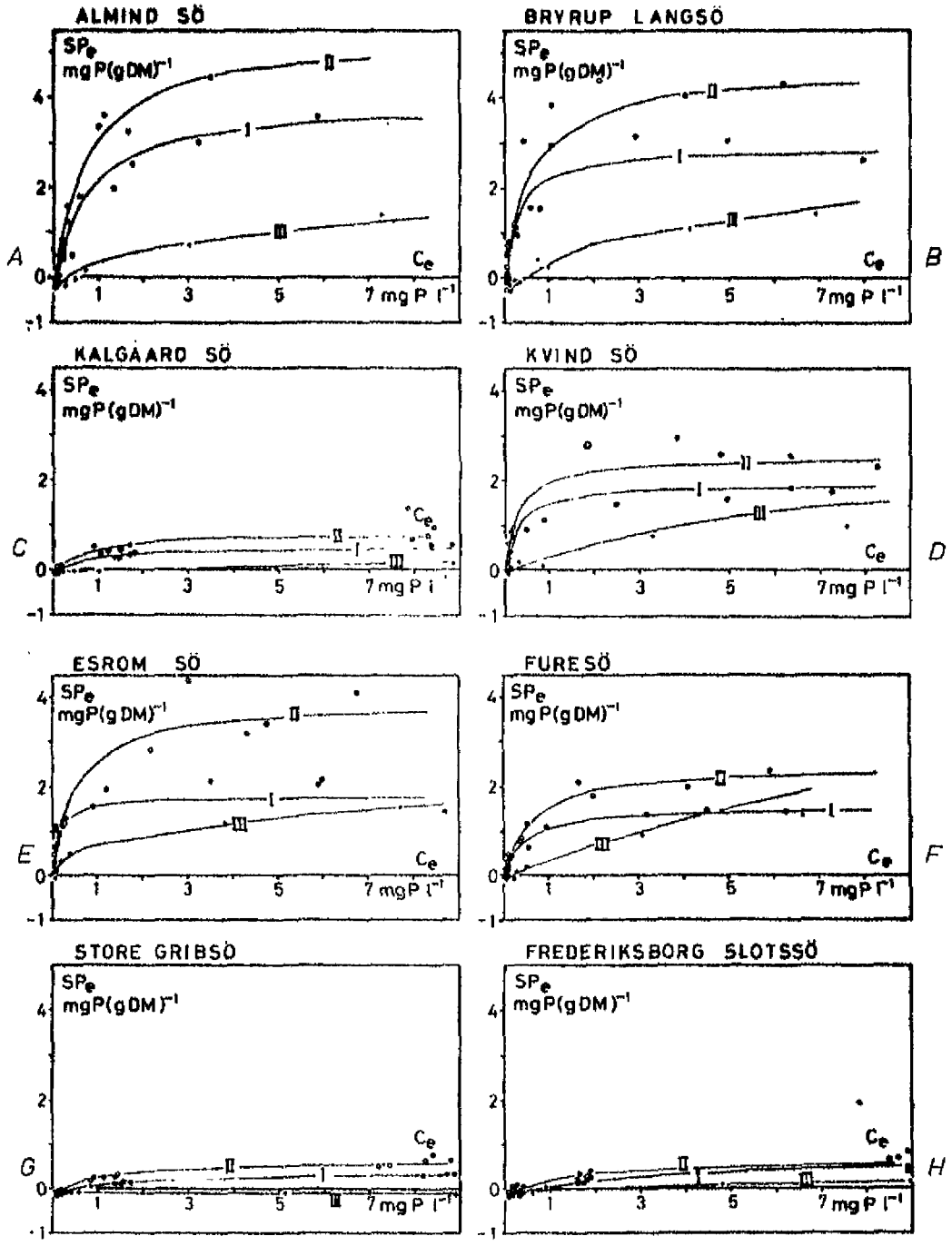

Results of sorption experiments and calculated isotherms. I: oxidized mud and demineralized water, II: oxidized mud and lake water, and III: reduced mud and demineralized water.

Figure 2.7.1 A -H

For chemical and physical data see table 2.7.1

		Almind sø	Bryrup Langsø	Kalgaard sø	Kvind sø	Esrom sø	Furesø	Store Gribsø	Frederiks-borg Slotssø
Area	km^2	0.5	0.4	0.1	0.1	17.2	9.2	0.1	0.2
Volumen	$10^6\ m^3$	4.5	2.1	0.5	0.3	212	114	0.5	0.6
Hydraulic input	$10^6\ m^3$	?	5	?	7	16	7	0	< 0.1
Lake type		oligo-mesotr.	eutr.	oligo	eutr.	eutr.	eutr.	humic	eutr.
Primary production	$gC\ m^{-2}y^{-1}$	80*	400	50	800	260	400	~ 50	560
P-loading	$gP\ m^{-2}y^{-1}$	0.1*	3-4	0.05*	11-17	0.04	3-5	0.05	0.1
Epilimnetic P-conc.	$\mu gP\ l^{-1}$	0-30	20-300	0-75	50-800	100-300	500-600	0-50	0-30
Lake water used for experiments	$\mu gP\ l^{-1}$	4	26	4	51	206	510	5	204
	pH	7.2	7.7	6.5	7.8	8.2	8.2	6.2	8.0

* estimated values

Chemical and physical data of the investigated lakes

Table 2.7.A

		Almind sø	Bryrup Langsø	Kalgaard sø	Kvind sø	Esrom sø	Furesø	Store Gribsø	Frederiks-borg Slotssø
Dry matter (DM)	%	9.9	7.6	8.0	9.3	6.8	20.9	13.9	6.5
Organic matter	$mg\ (gDM)^{-1}$	243	318	365	275	281	115	245	318
Ca	$mg\ (gDM)^{-1}$	5	9	5	14	101	167	7	88
Mg	$mg\ (gDM)^{-1}$	2.1	1.1	0.4	2.0	3,0	3.2	0.0	4.9
CO_3	$mg\ CO_3\ (gDM)^{-1}$	< 1	21	0	16	155	257	0	128
Total P	$mg\ P\ (gDM)^{-1}$	2.3	2.7	1.9	1.4	1.7	1.0	1.2	2.1
Total Fe	$mg\ Fe\ (gDM)^{-1}$	96.4	46.9	11.3	32.2	20.4	17.4	7.8	14.9
Oxalate-Fe	$mg\ Fe\ (gDM)^{-1}$	90.9	37.1	3.3	20.1	13.2	10.1	1.7	1.4
pH		6.7	5.4	5.9	6.3	8.2	7.8	6.7	8.3
Interstitial P_{o_1}	$\mu g\ P\ l^{-1}$	48	160	104	44	110	95	1560*	2310
Interstitial Fe^{++}	$mg\ Fe\ l^{-1}$	44.9	81.5	1.2	8.1	1.5	1.1	10.9*	1.6

* Humic-Fe-PO_4-complex

Chemical composition of sediments

Table 2.7.B

$$x = PSC \frac{C_e}{k + C_e} - NAP$$

(extended Langmuir isotherm)

x = phosphate sorbed
PSC = phosphate sorption capacity = adsorption maximum
C_e = equilibrium solution phosphate concentration
k = affinity constant
NAP = Natural Adsorbed Phosphate
and Freundlich isotherm: $x = K_{e(Ce)}P - NAP$

Table *Comparison of Langmuir and Freundlich isotherms.*

		pHe	n	NAP mg P (g DM)$^{-1}$	Langmuir isotherm			Freundlich isotherm		
					PSC mg P (g DM)$^{-1}$	k mg P l^{-1}	correlation coefficient r	K_F l (g DM)$^{-1}$	p	correlation coefficient r
Almind sø	I	6.7	19	0.651	4.56	0.62	0.99	—	—	0.96
	II	7.2	16		5.97	0.59	0.98	—	—	0.72
	III	6.1	8		—	—	0.95	0.97	0.335	0.93
Bryrup Langsø	I	5.5	19	0.418	3.32	0.25	0.99	—	—	0.93
	II	6.8	16		5.07	0.52	0.99	—	—	0.91
	III	5.9	8		—	—	0.14	0.68	0.592	0.98
Kalgaard sø	I	5.9	19	0.097	0.61	0.87	0.98	—	—	0.91
	II	6.3	16		0.91	0.81	0.99	—	—	0.96
	III	8.0	8		—	—	0.83	0.05	0.759	0.95
Kvind sø	I	6.3	19	0.152	2.10	0.29	0.99	—	—	0.93
	II	7.7	16		2.71	0.29	0.99	—	—	0.92
	III	7.6	8		—	—	0.21	0.47	0.655	0.83
Esrom sø	I	7.9	19	0.108	1.88	0.10	0.98	—	—	0.91
	II	8.2	16		4.03	0.48	0.98	—	—	0.93
	III	8.5	8		—	—	0.86	0.81	0.354	0.99
Furesø	I	7.9	19	0.152	1.68	0.38	0.99	—	—	0.95
	II	8.2	16		2.62	0.55	0.99	—	—	0.97
	III	8.9	8		—	—	0.67	0.49	0.762	0.94
Store Gribsø	I	6.5	19	0.140	0.55	1.45	0.99	—	—	0.94
	II	6.2	16		0.82	1.10	0.99	—	—	0.97
	III	6.8	8		—	—	0.62	0.14	0.495	0.95
Fredriksborg	I	7.9	19	0.166	0.99	3.66	0.82	—	—	0.90
	II	8.1	16		0.84	1.62	0.92	—	—	0.83
Slotssø	III	8.4	8		—	—	0.99	0.17	0.290	0.89

Table 2.7.1.C

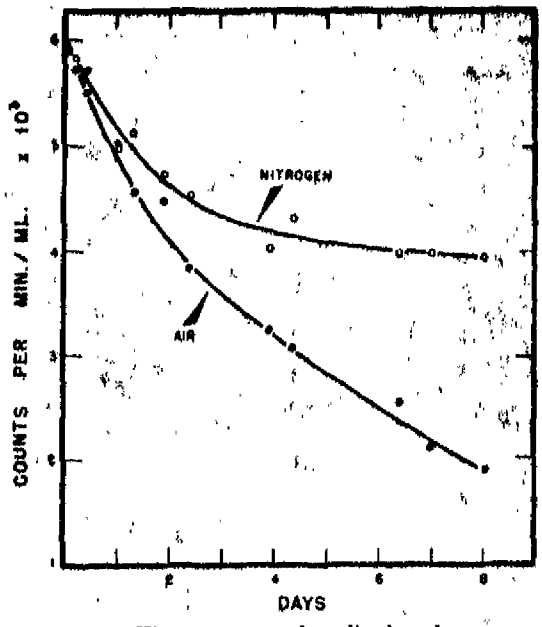

. The amount of radiophosphorus remaining in the water of antibiotic-treated Punchbowl mud-water systems under reducing (nitrogen) and oxidizing (air) conditions.

Figure 2.7.2

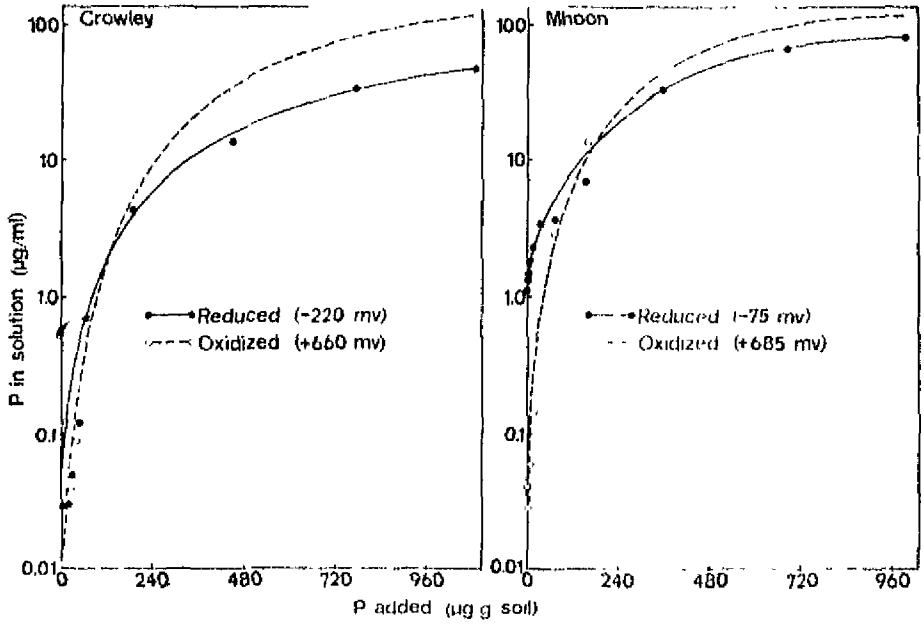

Amount of P remaining in solution 24 hours after addition to reduced and oxidized soil-water suspensions of Crowley and Mhoon soils. Redox potential measurements showed oxidizing values of +660 and +685 mv for the oxidized soils and reducing values of −220 and −75 mv for the reduced soils.

Table 2.7.3

Soluble P and extractable Fe under aerobic and anaerobic conditions. Values of Fe extracted are in micrograms per gram of soil; values of P are in micrograms per milliliter of solution.

Soil	pH	Fe extracted (µg/g)		Added P (µg/ml)	Soluble P (µg/ml)	
		Aerobic	Anaerobic		Aerobic	Anaerobic
Commerce	5.4	1,590	2,670	0	0.02	2.92
				100	79.2	66.1
Crowley	6.1	3,190	12,620	0	0.002	0.005
				100	40.8	6.7
Moreland	6.8	2,925	5,895	0	0.14	4.48
				100	48.2	13.0
Sharkey	6.5	3,025	3,910	0	0.03	1.17
				100	62.7	14.0

Table 2.7.2

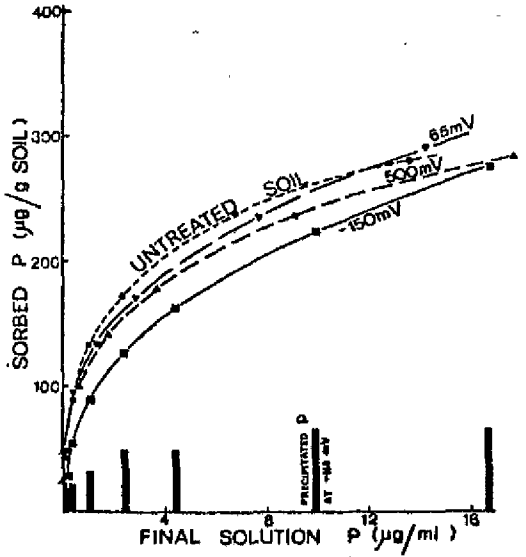

Effect of reduction on P sorption isotherms and P precipitation (histogram) at pH 5.

Effects of reduction on labile phosphate, phosphate sorption, and related variables at pH5.

Variable	Redox potential (mV)		
	-150	65	500
Solution composition (µg/ml)			
P concentration at zero added P	0.025	0.009	0.004
Fe concentration	560	5.1	0.2
Soil properties			
Labile P (µg/g)	29	76	28
P buffer capacity (ml/gx10^{-2})	11	152	57
P sorption energy (ml/µg P) k', k''	10	95	51
P sorption capacity (µg/g) x_m+x_m	519	387	391
pH after P sorption	4.9	4.8	4.8

Figure 2.7.4.A and table 2.7.3.A

1) only values of h' are given

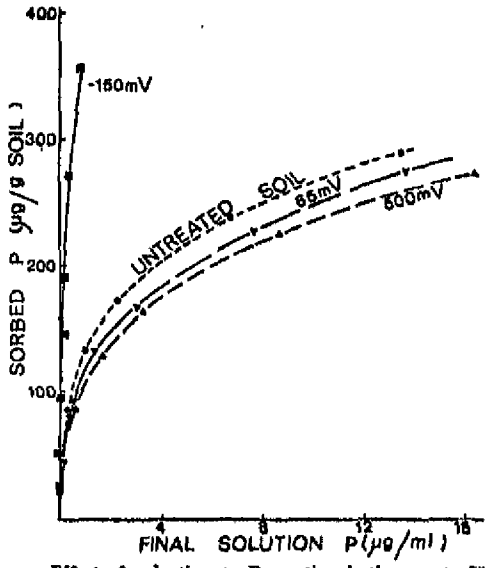

Effect of reduction on P sorption isotherms at pH 6.5.

Figure 2.7.4.B and table 2.7.3.B

Effects of reduction on labile phosphate, phosphate sorption, and related variables at pH 6.5

Variable	Redox potential (mV)		
	-150	65	500
Solution composition (µg/ml)			
P concentration at zero added P	0.017	0.004	0.006
Fe concentration	trace	0	0
Soil properties			
Labile P (µg/g)	255	40	18
P buffer capacity (ml/g x 10^{-1})	>300	100	24
P sorption energy (ml/µgP) h'	> 65	94	26
P sorption capacity (µg/g) $x'_m + x''_m$	>675	392	377
pH after P sorption	5.2	5.8	6.1

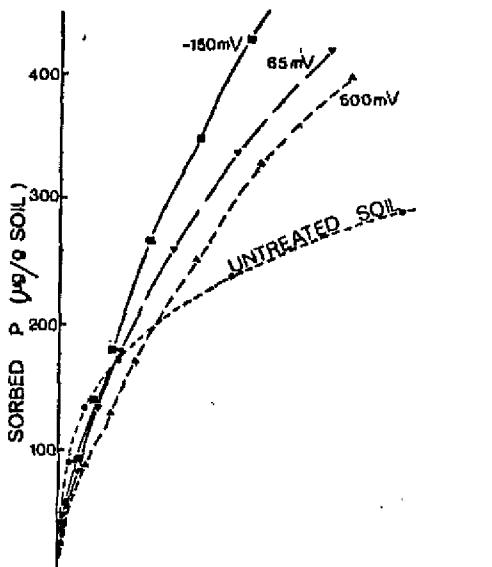

Effect of reduction on P sorption isotherms at pH 8.

Figure 2.7.4.C and table 2.7.3.C

Effects of reduction on labile phosphate, phosphate sorption, and related variables at pH 8.

Variable	Redox potential (mV)		
	-150	65	500
Solution composition (µg/ml)			
P concentration at zero added P	0.018	0.006	0.010
Fe concentration	trace	trace	0
Soil properties			
Labile P (µg/g)	17	8	12
P buffer capacity (ml/g x 10-2)	11	18	16
P sorption energy (ml/µgP) h'	14	41	42
P sorption capacity (µg/g) $x'_m + x''_m$	1,606	787	333
pH after P sorption	7.2	7.4	7.7

Calculated for low concentration range (<2.3 µg P/ml) of each isotherm

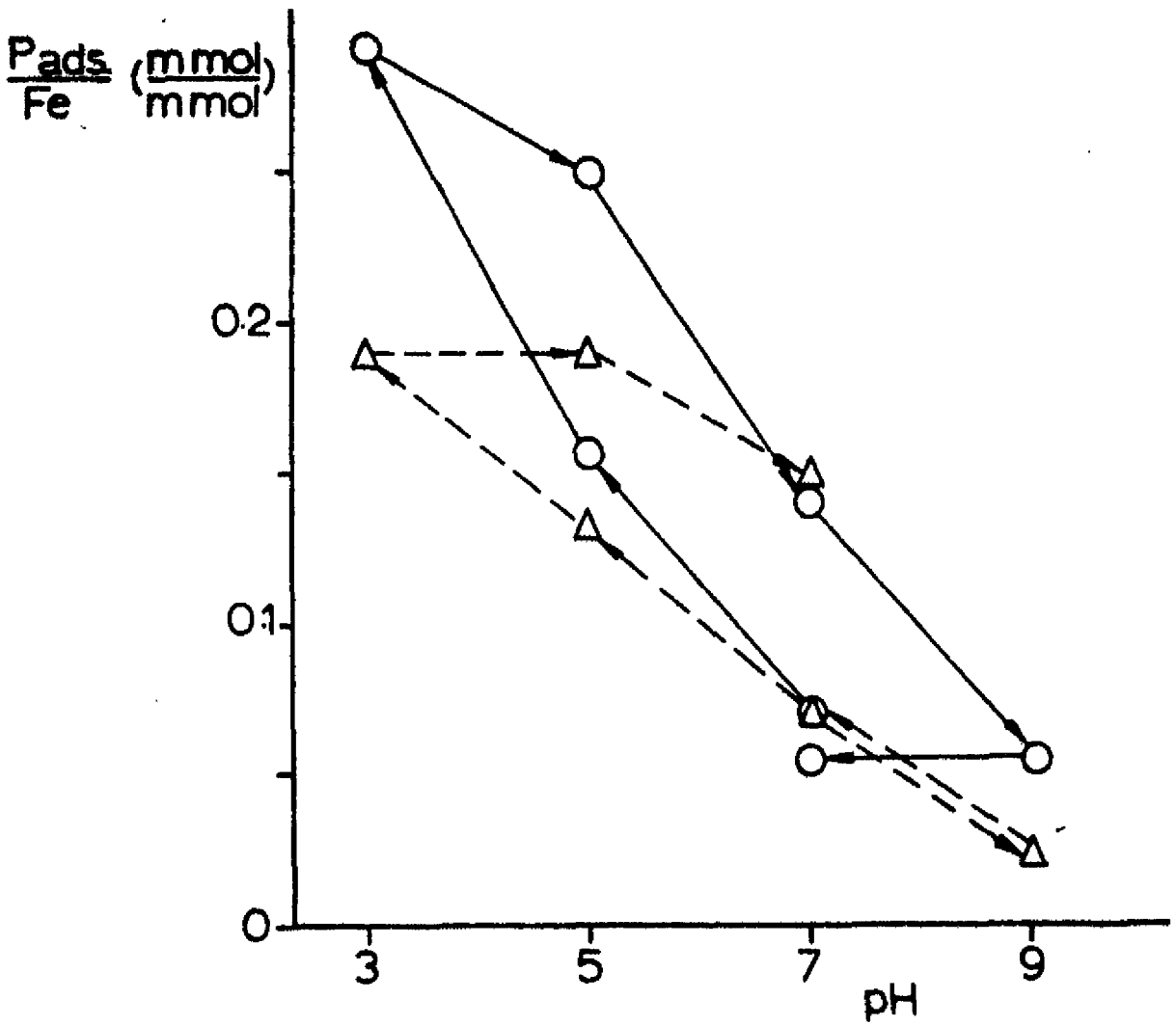

Figure 2.8.1 Hysteresis of phosphate adsorption on iron (III) hydroxide as effected by change in pH; (---) 1h intervals, (_____) 1 day intervals.

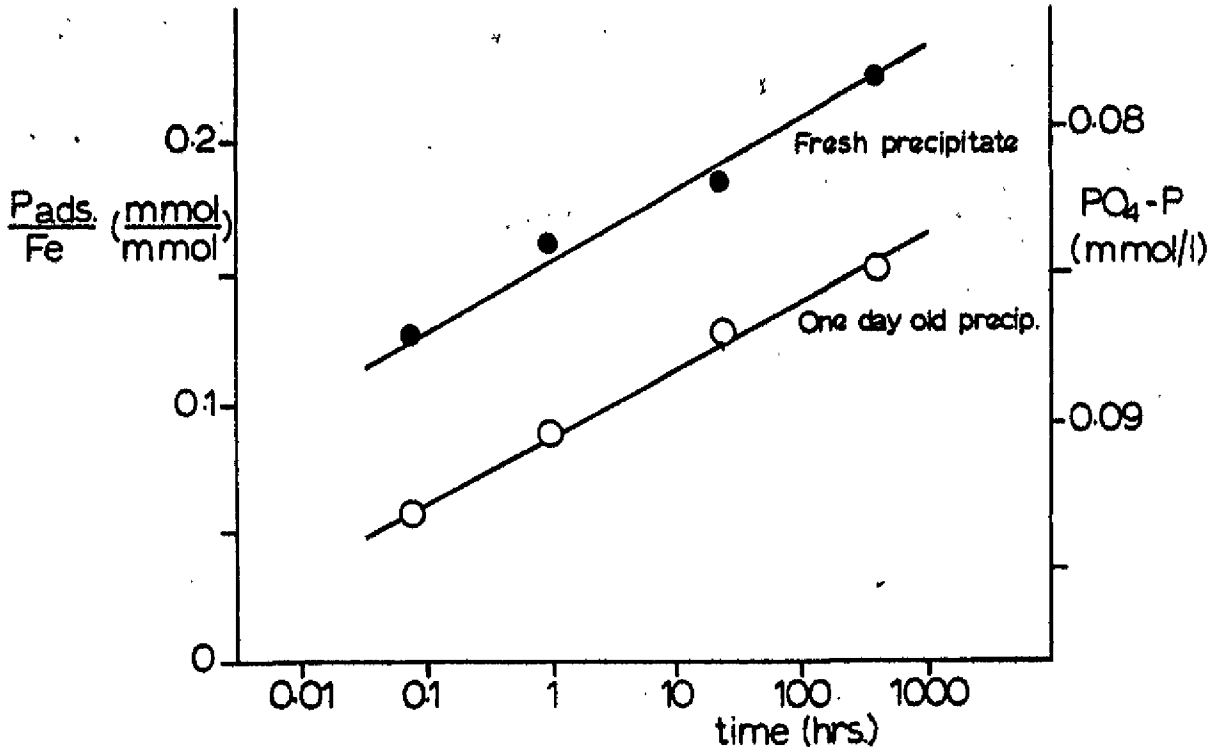

Figure 2.8.2 Phosphate adsorption by iron III hydroxices as function of time

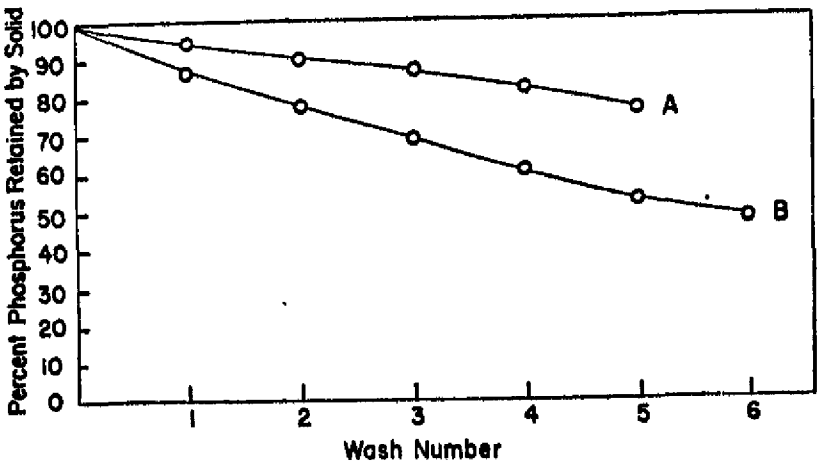

The effect of prior contact time on the desorption of phosphorus from solids. pH of wash 3·4 A. 4 days contact ; B.30 minutes contact.

Figure 2.8.3

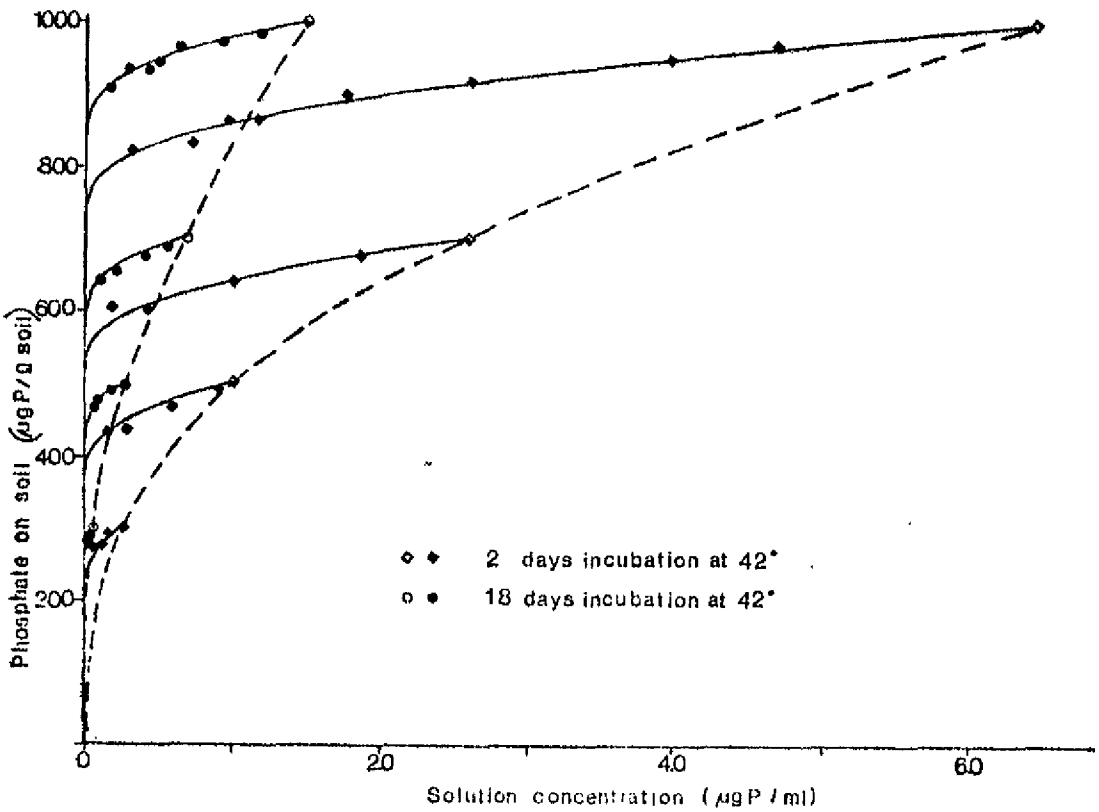

Relationship between the phosphate remaining on the soil and the solution concentration of phosphate. Open symbols and broken lines are from adsorption studies; solid symbols and solid lines are from desorption studies.

Figure 2.8.4

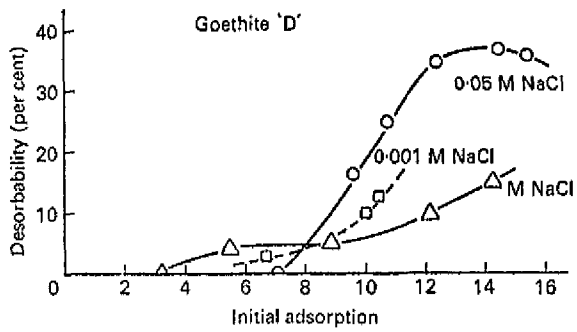

Desorbability of phosphate from goethite 'D' and gibbsite 'A', under conditions as shown on the figure, plotted against the initial amount adsorbed.

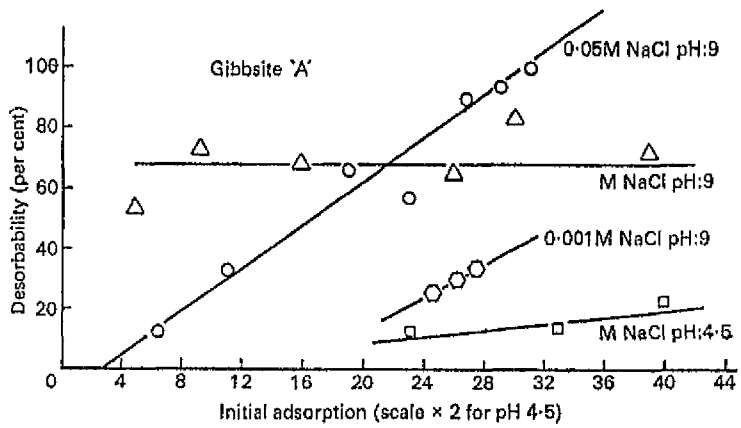

Desorbability of phosphate from gibbsite 'A' under conditions as shown on the figure, in relation to initial amount adsorbed.

Figure 2.8.5.A and B

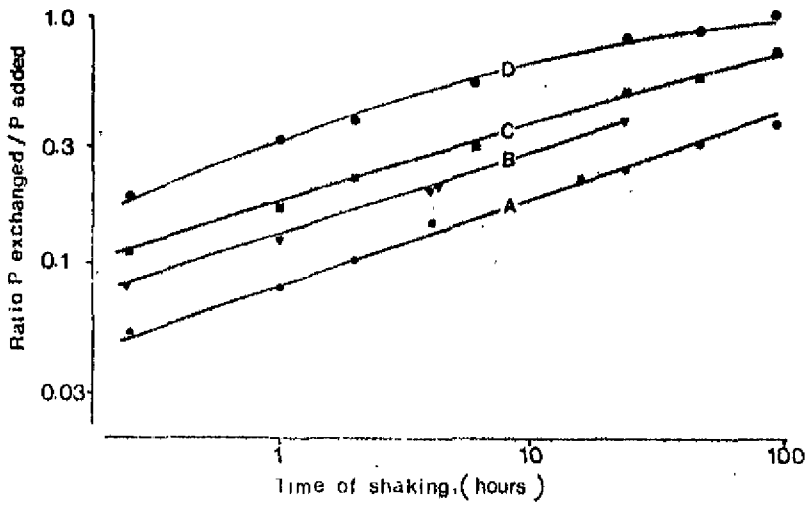

Effect of period of equilibration with labeled solution of four samples of soil which had been incubated with phosphate as specified below on the proportion of the added phosphate which exchanged. The incubation treatments and the fitted equations are:

Line A: Incubated for 220 days at 25°C
$\ln (P_t) = \ln (P) - 0.357 \ln (1 + 1138/t_t)$ $R^2 = 0.978$ $n = 32$
Line B: Incubated for 93 days at 25°C
$\ln (P_t) = \ln (P) - 0.342 \ln (1 + 358/t_t)$ $R^2 = 0.932$ $n = 19$
Line C: Incubated for 3 days at 35°C
$\ln (P_t) = \ln (P) - 0.311 \ln (1 + 232/t_t)$ $R^2 = 0.991$ $n = 7$
Line D: Incubated for 3 days at 17°C
$\ln (P_t) = \ln (P) - 0.375 \ln (1 + 20/t_t)$ $R^2 = 0.991$ $n = 7$

P_t (μg P/g soil) is the phosphate which exchanged; P (μg P/g soil) is the phosphate added; t_t hours is the period of equilibration. The lines drawn indicate values for the ratio P_t/P calculated from these equations.

Figure 2.8.8

p.o. box 177 2600 mh delft the netherlands